



Additive manufacturing of fatigue resistant materials: Challenges and opportunities



Aref Yadollahi^a, Nima Shamsaei^{b,*}

^a Department of Mechanical Engineering and Center for Advanced Vehicular Systems (CAVS), Mississippi State University, MS 39762, USA

^b Laboratory for Fatigue & Additive Manufacturing Excellence (FAME), Department of Mechanical Engineering, Auburn University, Auburn, AL 36849, USA

ARTICLE INFO

Article history:

Received 9 October 2016

Received in revised form 29 December 2016

Accepted 2 January 2017

Available online 4 January 2017

Keywords:

Additive manufacturing (AM)

Fatigue

Microstructure-property

Multiaxial loading

Review

ABSTRACT

This overview focuses on the current state of knowledge pertaining to the mechanical characteristics of metallic parts fabricated via additive manufacturing (AM), as well as the ongoing challenges and imminent opportunities in fabricating materials with increased fatigue resistance. Current experimental evidence suggests that the mechanical properties of laboratory AM specimens may not be representative of those associated with parts, due primarily to differences in geometry/size which influence the thermal histories experienced during fabrication, and consequently, microstructural features, surface roughness, and more. In addition, standards for mechanical testing methods, specimen design procedures, post-manufacturing treatments, etc., may need to be revised for AM parts. Standardizing the AM process may only be accomplished by strengthening the current understanding of the relationships among process parameters, thermal history, solidification, resultant microstructure, and mechanical behavior of the part. Having the ability to predict variations in mechanical behavior based on resultant microstructure, or matching the best conceivable properties of a part in accordance with the loading critical plane, are some possible solutions for making AM a more reliable means for producing functional parts. Developing microstructure-property models is arguably the first necessary step toward design optimization and the more efficient, accurate estimation of the structural integrity of AM parts.

© 2017 Elsevier Ltd. All rights reserved.

1. Introduction

According to the American Society for Testing and Materials (ASTM), additive manufacturing (AM) is defined as the “process of joining materials to make objects from three-dimensional (3D) model data, usually layer upon layer, as opposed to subtractive manufacturing methodologies” [1]. AM is a common term used to describe a group of advanced manufacturing technologies that create objects in a layer-wise method. There are different types of AM techniques depending on the feed stock form (e.g., powder versus wire), feeding system (e.g., powder bed versus blown powder), energy source (e.g., laser versus electron beam), and materials (e.g., metal versus polymer), etc. [2–4]. This overview is based on those that use the focused laser beam as a source of energy to melt metallic powder for forming a part. These types of AM methods can be classified in two main categories: (i) laser powder bed fusion (L-PBF), in which a bed of powder serves as the feeding system, such as selective laser melting (SLM), and (ii) direct laser deposi-

tion (DLD), which employs a blown powder system, such as laser engineered net shaping (LENS) [2].

These new manufacturing techniques have provided new avenues for fabricating net-shaped parts, and even assemblies, with complex geometries that traditional manufacturing methodologies are unable. New developments in AM processes, along with innovations in advanced materials, have enabled more unique approaches for product development, manufacturing, and supply chain management [5,6]. Since AM has less geometrical constraints, industries will benefit from AM by finding new design paradigms for achieving lighter and cleaner products, as well as shorter lead times with lower costs. Moreover, AM can streamline the manufacturing and assembly process since assemblies can be consolidated into a single additive part, reducing the total number of parts and overall cost [2–4,7].

Additive manufacturing perhaps has the most appeal to industries targeting low volume production of highly customized parts for specific applications, especially in the medical arena [8]. Surgical instruments and patient/injury-specific implants can be generated via AM for reducing patient wait times and accelerating their post-implant healing. Via AM, more individualized medical equipment can be generated and delivered more rapidly at a reasonable

* Corresponding author.

E-mail address: shamsaei@auburn.edu (N. Shamsaei).

Nomenclature

k	material constant	$\Delta\sigma/2, \sigma_a$	stress amplitude
N_f	number of cycles to failure	ε	axial strain
$2N_f$	number of reversals to failure	σ	axial stress
R_a	surface roughness	$\sigma_{n,max}$	normal stress acting on the plane of maximum shear strain
R_ε	strain ratio	σ_y	monotonic yield stress
R_σ	stress ratio		
$\Delta\gamma_{max}/2$	maximum shear strain amplitude		
$\Delta\varepsilon/2, \varepsilon_a$	strain amplitude		

price [5,6]. Beside these, AM provides the ability of remote manufacturing and repair (in space, at sea) on demand as well as manufacturing of functionally-graded parts. Hence, AM has gained considerable attention from various industries, such as aerospace and biomedical, to fabricate functional service parts. However, the full potential of AM to provide new means for manufacturing load bearing (i.e. structural) parts is not yet fully realized [9].

The main challenge against the continued adoption of AM by industries is the uncertainty in structural properties of their fabricated parts [3,4,9]. This uncertainty arises due to AM parts possessing microstructural heterogeneities and randomly dispersed defects [9]. In addition to the variation in as-received powder characteristics, building procedure, and AM systems, this challenge is exacerbated by the many involved process parameters, such as laser power, laser speed, layer thickness, etc., which affect the thermal history during fabrication [3,4,9]. Thermal history (i.e. melt pool temperature, thermal gradient, cooling rate, cyclic reheating) in AM process affects the microstructural details, such as grain size, morphology, and texture; defect type, size, and spatial distribution; residual stress, etc., and consequently, mechanical behavior of fabricated part [9].

Although significant research effort has been devoted to parameter optimization/control to achieve more uniform microstructure in AM parts [2,10], undesirable consequences of this manufacturing method on material properties are inevitable, and overcoming this challenge is still an open issue [9]. In addition, even under fixed, optimized process parameters, any change in build parameters, such as part size and build orientation, may cause variation in microstructural, and consequently, mechanical characteristics [11,12]. As a result, there are still significant gaps to fully understand and establish the relationship between the process, structure, property, and performance of AM parts [13].

In this overview, the fatigue characteristics and related challenges inherent to metallic parts fabricated via laser-based additive manufacturing are discussed. It should be noted that the goal of this paper is not to include all the existing studies related to AM, but to provide an overview mostly based on many authors' research to emphasize the important and imminent challenges pertaining to characterizing the fatigue behavior of AM metals. There are definitely other related topics to the structural integrity of AM parts, such as residual stresses, very high cycle fatigue behavior, and more, that are not discussed in this overview.

The organization of this paper is as follows. Fatigue behavior of AM materials and their comparison with conventionally-built counterparts are described in Section 2. Next, the effects of size, time interval and geometry on mechanical behavior and microstructural properties of AM parts are presented in Section 3. Section 4 discusses anisotropy in mechanical properties (i.e. tensile and fatigue), imposed by part's build orientation during AM process. The effect of surface finish on fatigue resistance and failure mechanism of AM parts is described in Section 5. Some opportunities in additive manufacturing of more fatigue resistant materials

are discussed in Section 6. Finally, a summary of this manuscript along with some conclusions is provided in Section 7.

2. Fatigue behavior and failure mechanisms

In general, the mechanical properties under static loading, including tensile, compressive, hardness, etc., of AM parts are comparable to their conventionally-fabricated forms [14]. This is primarily due to the fact that AM parts experience relatively high cooling rates during their fabrication, resulting in finer microstructure as compared to their conventionally-fabricated counterparts [4,9,15,16]. Although there exists a number of works focused on the characterization of AM parts, their mechanical behavior (including the trustworthiness and durability) is still not well understood [9].

A major concern for metallic AM parts in application is their performance under cyclic loading, i.e. their fatigue resistance – a common mode of mechanical failure in many engineering structures [9,11,17]. Contrary to failures that occur under static loading, failure by fatigue is mostly a local phenomenon driven by impurities and microstructural heterogeneity – traits descriptive of metallic parts fabricated using current AM technology [9,11,17]. Therefore, improving the trustworthiness and durability of engineering parts fabricated via AM cannot be achieved without a thorough understanding of the fatigue damage process, failure mechanisms, and more specifically, their relationships with the microstructure of AM materials.

Due to variations in post-manufacturing processes, material feedstock, specimen types (round versus flat), testing modes (strain-controlled versus force-controlled), etc., it is difficult to make direct comparisons between fatigue data obtained from AM materials and those obtained from conventionally-built parts of the same material as reported in the literature. However, to facilitate general discussion, some fatigue data related to AM parts such as DLD Ti-6Al-4V (as-built without any heat treatments) [18], L-PBF 17-4 PH stainless steel (SS) (heat treated) [11], and L-PBF Inconel 718 (hot isostatic pressed and heat treated) [19] are compared with those of corresponding wrought materials at room temperature reported elsewhere [20–23]. These data are presented in Fig. 1. As seen in this figure, AM materials exhibit significantly shorter fatigue lives and lower high cycle fatigue (HCF) strength as compared to their corresponding wrought material form. Other studies [15,24–26] have also reported lower fatigue resistance for AM parts regardless of the manufacturing method and material type. It is well established that the surface roughness of parts can adversely affect its fatigue behavior [17]. Hence, in order to provide a more reasonable and unbiased comparison between the AM parts, which typically possess significant surface roughness, with fatigue data corresponding to their wrought material forms, data pertaining to AM parts in their machined and/or polished surface conditions were selected for this comparison.

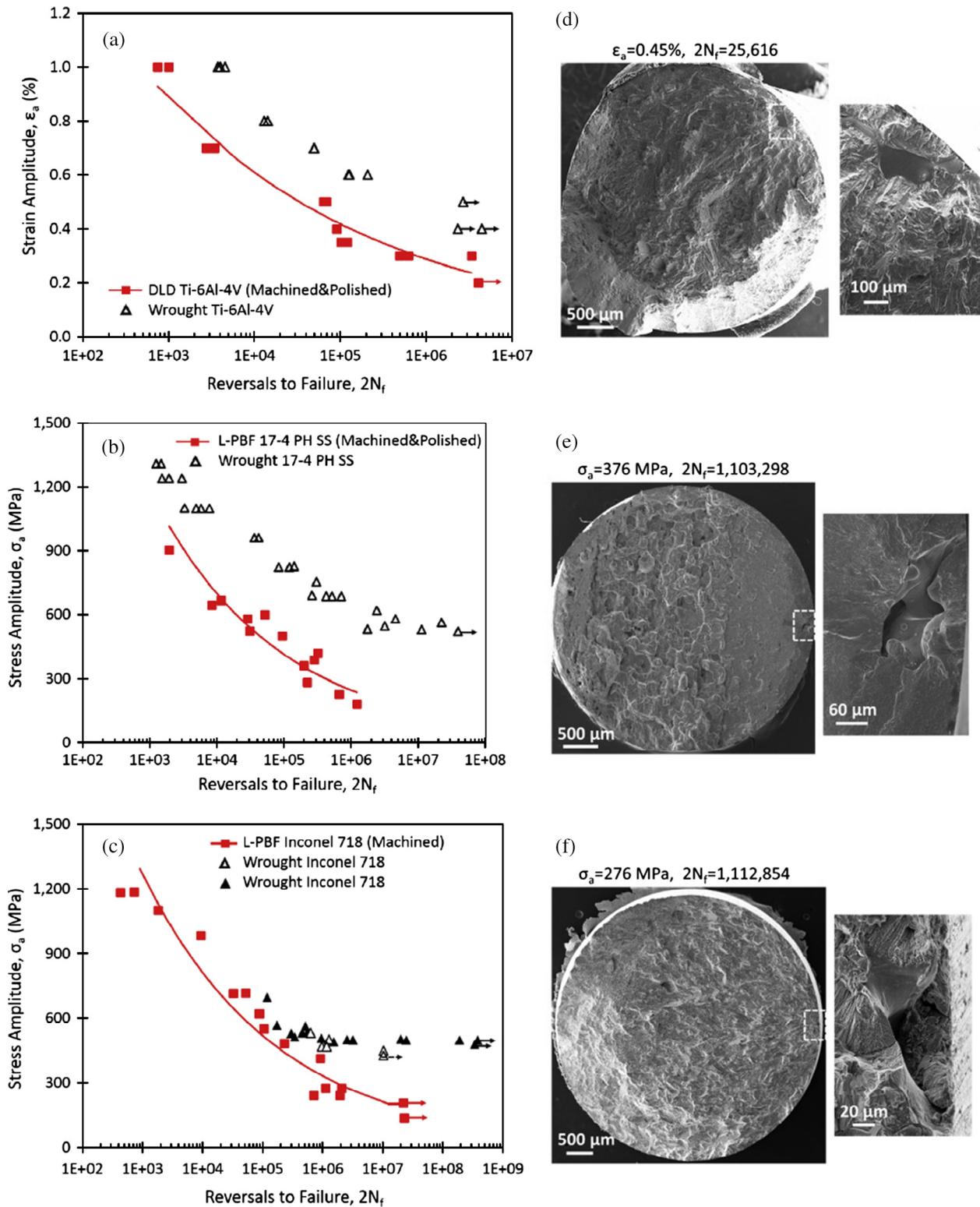


Fig. 1. Comparison of fully-reversed uniaxial fatigue data of (a) DLD Ti-6Al-4V [18], (b) L-PBF 17-4 PH SS [11], and (c) L-PBF Inconel 718 [19] to wrought materials [20–23], at room temperature. Fatigue fracture surfaces and crack initiation sites of (d) DLD Ti-6Al-4V [18], (e) L-PBF 17-4 PH SS [11], and (f) L-PBF Inconel 718 [19] specimens.

Considering the fact that the ultimate tensile strength of AM materials, investigated previously by the authors [11,18,19], was almost similar to that of wrought counterparts, the shorter fatigue life of AM materials – especially in high cycle fatigue (HCF) – can be explained by the presence of defects, which can serve as crack initiation sites. Fig. 1 presents the crack initiation sites for the

previously-investigated DLD Ti-6Al-4V [18], L-PBF 17-4 PH SS [11], and L-PBF Inconel 718 [19] specimens. Fractography of the failed specimens reveals that, regardless of the manufacturing method and material type, cracks tend to initiate from voids induced during the powder-based AM process, as shown in Fig. 1 [11,18,19].

Further microstructural examination and fractography of AM materials have revealed different types of defects, such as voids and particles, as the main sources of damage [11,18,19]. Voids can be classified as *pores* or *un-melted regions* (i.e. weak metallurgical bonding between layers, so-called lack of fusion). The existence of pores is predominantly attributed to entrapped gas, a result of vapor recoil during melt pool formation or non-ideal formation of powders during their fabrication. Un-melted regions within AM parts form due to insufficient fusion and/or low laser penetration depth during fabrication. Pores are typically small in size and possess a spherical-shape, whereas un-melted regions are irregularly-shaped, and most importantly, slit-shaped. Particle inclusions may be classified as *partially- or un-melted powder particles*, caused by ineffective fusion, and *primary/secondary phase particles*, formed during solidification.

In wrought materials, slip bands and microstructural weak points (e.g., microstructural defects and grain boundaries) typically compete together for initiating cracks by providing local plastic deformation under cyclic loading. However, current analysis of the fatigue fracture surfaces reveals that cracks initiate from voids located closer to the surface of AM parts, which seems to be the most life limiting failure mechanism for AM materials [11,18,19,26]. Such surface voids provide the required stress concentration to initiate a crack at a lower number of fatigue cycles.

Location, shape, and size of voids have been found to be the main contributor for the larger scatter in HCF data of AM materials [11,18,19,26]. Since the crack initiation stage dominates the total fatigue lifetime in HCF, sensitivity to defects is more pronounced when compared to the low cycle fatigue (LCF) regime, where the crack propagation stage typically dominates the total fatigue lifetime [17]. Although the mechanisms for crack initiation depend on the material as well as applied stress/strain level (i.e. LCF versus HCF), voids with larger size, more irregular shape, and closer to the surface are found to be more detrimental to fatigue resistance due to their provision of higher stress concentrations [11].

Results have shown that for most cases, the failure mechanism of AM materials is more affected by void location as opposed to its shape or size, as crack initiation sites are observed to be closer to the specimens' surface [11,19,26,27]. In fact, an AM part consisting of high intra-part void density (i.e. large voids or cluster of voids), located far from the surface, still does not exceed the dominating and detrimental influence of a near-surface void with regards to crack initiation [27]. Surprisingly, fatigue experiments on DLD NiTi (also known as Nitinol) [26] have demonstrated that, regardless of the location, shape, and size of the microstructural defect, fatigue life is always shorter for the duplicate specimen with the higher stress response (i.e. the average net section stress). This observation indicates that the maximum stress level may be the most influential factor on the fatigue behavior of additively-manufactured superelastic NiTi [26,28].

Hot isostatic pressing (HIP) is often considered as the most effective post-manufacturing treatment available for remedying process related defects of AM parts and improving their fatigue performance [24,29]. Via HIP, it is possible to homogenize the microstructure of AM parts while also densifying and stress relieving their matrix, as HIP uses the combined action of high pressure and temperature. Several studies have shown that employing HIP on AM Ti-6Al-4V can significantly improve its fatigue resistance, resulting in comparable fatigue strength relative to their wrought counterparts [24,30,31]. However, these findings cannot be generalized for other AM materials without taking into account other material aspects, such as void/microstructure characteristics and failure mechanisms.

For instance, a study performed by Leuders et al. [32] on 316L SS, fabricated via an L-PBF system, showed distinct fatigue behavior after HIP, as presented in Fig. 2. As it may be seen, in contrast to

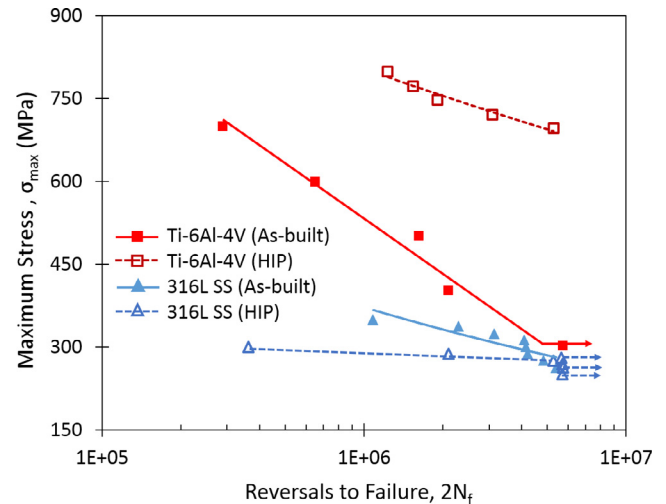


Fig. 2. Comparison of fully-reversed ($R_\sigma = -1$) fatigue stress-life data for L-PBF Ti-6Al-4V and L-PBF 316L SS in as-built and HIP conditions [32].

Ti-6Al-4V, L-PBF 316L SS in its 'HIPed' condition demonstrates lower fatigue resistance relative to its as-built counterpart in shorter life regimes. This is due to the fact that the failure mechanism of Ti-6Al-4V is still dominated by the remaining voids after employing HIP [32], while damage evolution in 316L SS under cyclic loading is more strongly affected by its monotonic strength, which can actually be reduced through HIP [32]. In addition, 316L SS has a very high ductility (>50%), which can possibly accommodate an increased stress field imposed by defects; thus, the influence of HIP on the fatigue strength is less effective as compared to that of Ti-6Al-4V [32]. It should be noted that no further heat treatments were performed after HIP was done on either material.

The fatigue resistance of L-PBF Inconel 718 specimens [19], as presented in Fig. 1c, also possesses a relatively low HCF resistance while in the HIPed condition ($1163 \pm 10 \text{ }^\circ\text{C}$ and $\sim 102 \text{ MPa}$ for 3 h). Analysis of the HCF fracture surfaces of L-PBF Inconel 718 has revealed crack initiations from large un-melted regions (>100 μm) adjacent to the specimens' surfaces [19]. The L-PBF Ti-6Al-4V investigated by Leuders et al. [27] also showed the presence of large voids (>72 μm) after HIP, and these voids were found to serve as fatigue crack initiation sites. These findings suggest that voids inside AM parts cannot always be suppressed by employing HIP. In fact, in addition to the parameters chosen for HIP (i.e. pressure, temperature, and time), closure of a void is dependent on the encapsulated gas inside of it [30].

The laser-based AM process takes place inside a chamber filled with an inert, protective gas, e.g., argon, to avoid oxidization of the fabricated material at elevated temperatures. The complete suppression of process-sourced voids in AM parts fabricated in an inert atmosphere may be difficult to achieve given the low solubility of common inert gases in the metal matrix [30,33]. Nevertheless, the HIP process can still improve the durability and HCF performance of AM parts by decreasing the size of voids and smoothing their sharp angles, as well as fusing any un-melted particles.

3. Effects of size, geometry, and process time interval

In AM methods, any change in the size, geometry, or number of fabricated parts on the build plate may significantly affect the final product properties (micro- and macro-structural) [2,12]. Therefore, for parts with complex geometries, the possibility of achieving a homogenous microstructure and defect distribution is debatable

given the current state-of-the-art in AM technology. More importantly, mechanical data as collected from small laboratory specimens may not be truly representative of actual parts of the same material and process. Thus, establishing process-structure-property-performance relationships for various AM materials and processes is vital for reducing uncertainty in performance of the fabricated parts.

The primary reason for variation in properties as a result of a change in specimen/part size or geometry is related to the thermal histories experienced during fabrication, which can be affected by any change in the inter-layer time interval, i.e. the amount of time taken for the laser to finish one layer and start depositing the next layer [12]. The inter-layer time interval can also vary with the number of parts fabricated on a build plate, which is important for scenarios in which one seeks to maximize the number of parts fabricated per build operation. Therefore, even under constant laser process parameters and scanning pattern, different inter-layer time intervals are inevitable as one changes the size or number of parts on the build plate. As a result, distinct thermal histories, and consequently, various microstructural details including grain size, phase fraction, and defect size and distribution may be obtained by varying the inter-layer time intervals [12].

The effect of inter-layer time intervals during DLD [12] and L-PBF [34] processes on the properties of fabricated samples has been recently investigated. This was achieved by varying the number of samples fabricated on a build plate [12,34], as shown in Fig. 3. In one set, a single cylindrical rod was fabricated on the build plate (single-built), as shown in Fig. 3a, while for the other set, multiple rods were fabricated on the build plate together (multi-built), as shown in Fig. 3b. As a result, the samples of each set experienced different inter-layer time intervals and distinct thermal histories (i.e. heating/cooling rates) during fabrication.

For single-built 316L SS samples fabricated via DLD, the inter-layer time interval was approximately 10 s, and the multi-built samples experienced an inter-layer time interval nearly 10x as large, i.e. ~ 100 s [12]. Microstructural investigations revealed distinct porosity and grain size for the DLD 316L SS samples of the two sets, as presented in Fig. 3c [12]. Samples with longer inter-layer time intervals (i.e. multi-built) contained a finer microstructure due to higher cooling/solidification rates along each layer (~ 60 μm in average). Conversely, samples with shorter inter-layer time intervals (i.e. single-built) experienced lower cooling rates and higher bulk temperature, resulting in a coarser microstructure (~ 140 μm in average) [12]. In addition, longer inter-layer time intervals were found to diminish the laser penetration depth, or heat affected zone size, due to colder initial layer temperatures, which impacted the degree of previous layer remelting. Due to this lower laser penetration depth, previously-deposited layers displayed lack of fusion traits, as such layers could not become sufficiently molten to achieve effective metallurgical bonding. This allowed the formation of un-melted regions between layers. As a result, voids were found to be more prevalent in the multi-built samples relative to the single-built ones, as shown in Fig. 3c [12].

Multi-built specimens fabricated via DLD were found to exhibit higher Vickers hardness, compressive yield, tensile yield and ultimate strength values as compared to their single-built counterparts [12]. This is attributed to the longer inter-layer time intervals utilized for the multi-built specimens, leading to higher cooling rates, and consequently, finer microstructure. Engineering tensile stress-strain curves of DLD 316L SS for the single-built and multi-built sets are shown in Fig. 3d [12]. It may be seen that the elongation to failure of the multi-built specimens is significantly lower than that of the single-built set, due to the higher level of porosity and finer microstructure. Moreover, since slight oxidization is somewhat unavoidable for the employed DLD pro-

cess, oxide particles were observed more frequently on the tensile fracture surface of multi-built specimens, as such specimens experienced longer exposure times during the manufacturing process relative to the single-built ones [12]. These features may also justify the observed lack of ductility for the multi-built specimens.

The authors herein have also evaluated the effect of process time intervals on fatigue behavior of DLD Ti-6Al-4V [35]. The results have demonstrated a significant difference in fatigue performance between single-built and double-built specimens in various fatigue life regimes [35]. Double-built Ti-6Al-4V specimens showed lower fatigue strength as compared to their single-built counterparts, mostly due to the presence of more voids serving as crack initiation sites. In addition, the coarser microstructure of the single-built specimens may have caused a higher resistance to crack propagation by providing a more tortuous path for crack growth, mostly in the low cycle regime [35].

A similar study suggests that the mechanical properties of parts fabricated via L-PBF are less sensitive to variations in the inter-layer time interval [34]. As shown in Fig. 4, differences in tensile and compressive strengths, as well as elongation to failure under tension, between single-built and multi-built sets of L-PBF 17-4 PH SS are not significant [34]. Relative to DLD, L-PBF can provide for significantly higher laser scanning speeds (~ 10 – $100\times$ faster) and lower layer thicknesses ($\sim 10\times$ smaller), and most importantly, the part is surrounded by powder during the build. The surrounding powder behaves as an insulator to heat transfer, and since L-PBF parts are not exposed fully to the environment during the build, the cooling rates are less surface area dependent. In addition, the powder feeding mechanism in L-PBF processes causes an extra inter-layer delay (~ 15 s) – due to the time that it takes to spread a new powder layer – decreasing the difference in the total inter-layer time between single-built (~ 20 s) and multi-built (~ 55 s) specimens. Spreading a new powder layer over the previously-built material also allows the accumulated heat in the parts to reduce due to heat transfer with the cooler, fresh powder layer, which results in various part assemblies having more similar thermal histories. Nevertheless, variation in lower length-scale (micro-level) properties is still likely to occur for parts fabricated via L-PBF. Therefore, it can be expected that the inter-layer time interval variations during L-PBF will affect the fatigue behavior, which is a more local phenomenon relative to monotonic properties.

4. Effect of build orientation

The orientation in which AM parts are built (i.e. build orientation) may greatly affect defect directionalities (i.e. aspect ratio in shape), and thus, generates and dictates their anisotropic structural response, especially in tensile strength, elongation to failure, and fatigue resistance [11,24,29,36–39]. In addition, the anisotropy may also be resulting from changes in the thermal history during fabrication (i.e. cooling rate and cyclic re-heating from subsequent layers), which affect microstructural details (i.e. grain size, phase fraction, defect size, type and distribution, etc.) [11].

It has been found that 17-4 PH SS, fabricated via an L-PBF method in the vertical and horizontal orientations, reveal anisotropy in tensile strength, elongation to failure, and fatigue resistance, as shown in Fig. 5 [11]. From Fig. 5, it may be seen that horizontally-built specimens in their as-built condition exhibit higher monotonic tensile strength, fatigue resistance, and elongation to failure relative to the L-PBF parts built vertically. The L-PBF 316L SS specimens have found to also possess higher fatigue strength when built horizontally as compared to either vertically or diagonally (45° with respect to the build plate) [40]. Other studies in the literature have reported similar results, with horizontally-built specimens possessing higher tensile strength

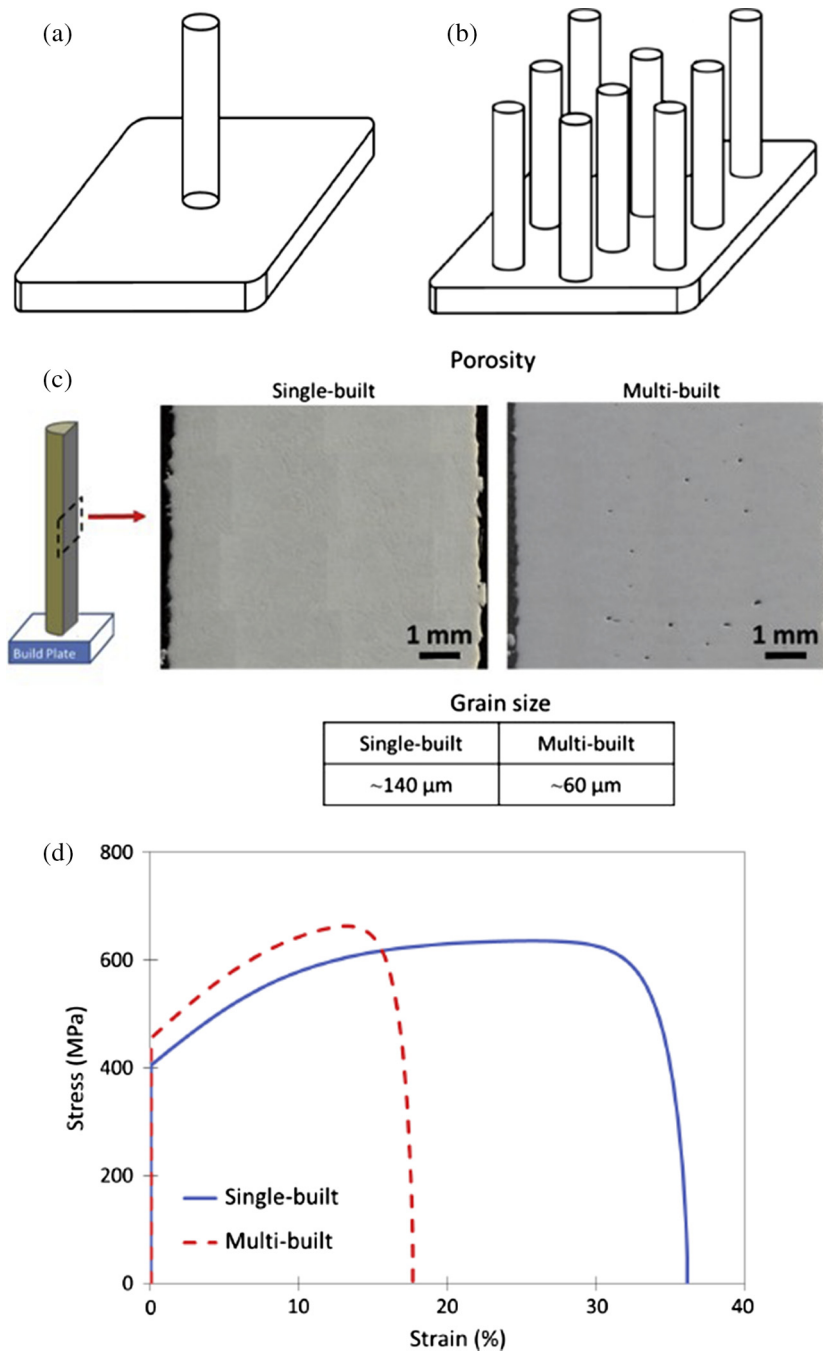


Fig. 3. Schematic of fabricated samples with different inter-layer time intervals including (a) single-built and (b) multi-built, (c) porosity distribution and measured grain size for single-built and multi-built samples at the middle region [12] and (d) engineering tensile stress-strain curves of DLD 316L SS for single-built and multi-built specimens [12].

and fatigue resistance relative to those fabricated in other orientations [11,24,29,36,37,41].

Mower and Long [41] recently demonstrated higher fatigue strength for horizontal L-PBF 17-4 PH SS specimens as compared to diagonal specimens. Likewise, enhanced fatigue resistance was observed for Ti-6Al-4V specimens fabricated via either L-PBF or DLD in the horizontal orientation, as compared to their vertically-built counterparts [24,29]. These findings indicate that a part's build orientation strongly affects its fatigue resistance independent of the material type and manufacturing method (i.e. L-PBF or DLD).

In general, as-built AM parts inherently consist of anisotropic microstructure due to an uneven thermal history and directional

heat transfer that the parts experience during fabrication [42,43]. Microstructural features, including grain size, grain morphology, and crystallographic orientation, affect the fatigue performance and failure mechanism of the part, especially pertaining to crack initiation and short crack growth. Therefore, the effects of microstructural features, as driven by the thermal history during the AM process, need to be considered when investigating the anisotropic behavior of AM parts [9].

In the absence of voids and inclusions, slip bands usually drive crack initiation in metallic materials [44]. In general, finer microstructures provide better crack initiation resistance than coarser microstructures due to a higher density of slip bands – when crack initiation occurs in slip bands within grains [45]. Addi-

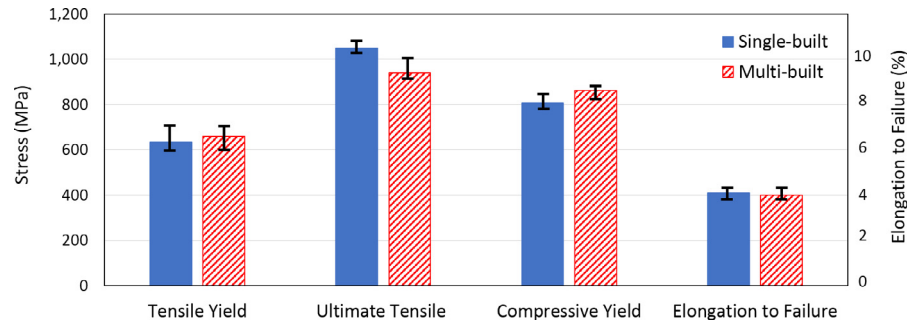


Fig. 4. Comparison of tensile and compressive strengths as well as elongation to failure for L-PBF 17-4 PH SS in single-built and multi-built conditions [34].

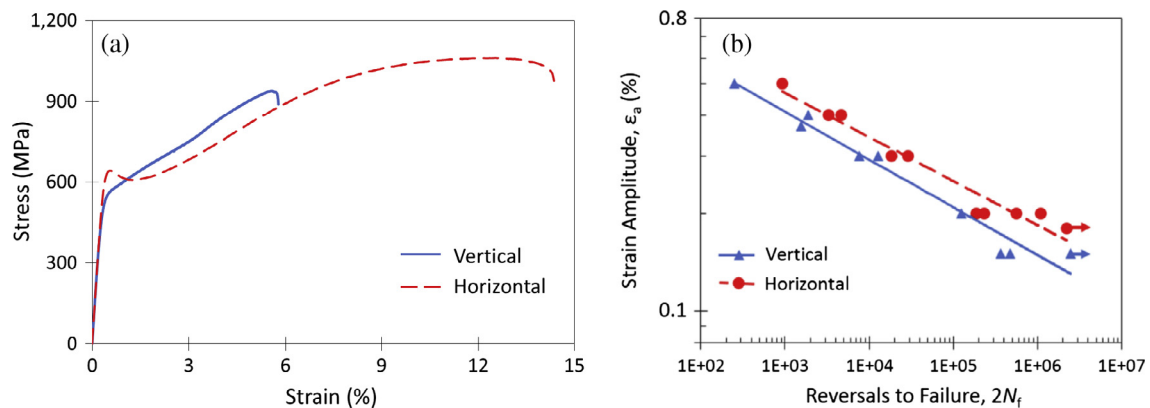


Fig. 5. (a) Engineering stress–strain curves, and (b) fully-reversed ($R_e = -1$) strain–life fatigue experimental data for vertically- and horizontally-built L-PBF 17-4 PH SS in as-built condition [11].

tionally, fatigue crack initiation of textured materials is controlled by the orientation of the active slip system(s) with respect to the loading direction(s) – i.e. maximum shear stress [46]. For instance, higher fatigue strength has been reported for Ti-6Al-4V when the maximum resolved shear direction is perpendicular to basal planes, where the easiest and most common slip systems, basal slip, reside in this alloy [47–51]. Crystallographic orientations of the adjacent grains may also act as a barrier for short crack growth [52,53]. The crack path deflection across a grain boundary is strongly influenced by the relationship between the grain orientations of neighboring grains [54]. Therefore, high-angle grain boundaries act as an effective barrier to transgranular short crack growth. Crack growth may be retarded/arrested when none of the available slip systems are oriented closely [45,53,55].

Grain size and morphology can also influence intergranular fatigue crack growth, leading to anisotropy in fatigue performance of AM materials. Typically, coarser grains can provide better crack growth resistance due to their larger grain boundaries, causing larger crack deflections [17,45,56]. In addition, anisotropic grain growth, leading to an elongated grain morphology, may affect crack growth for different loading directions. Elongated grains (i.e. columnar) typically form during the AM process in the direction of solidification, which tends to be near-parallel with the building direction [12,16,37,57]. In cases where loading is perpendicular to the building direction (i.e. the elongated direction of grains), cracks typically grow parallel to the building direction, as shown in Fig. 6a, and therefore, they experience less deflection in the path, leading to a lower crack growth resistance. On the other hand, a higher crack growth resistance can be expected when the crack growth is perpendicular to the building direction, as shown in Fig. 6b; such cracks experience a more tortuous and deflective crack path [37,56].

It is expected that post manufacturing heat treatments, such as solution/homogenizing annealing, will remove the aforementioned microstructural directionality or heterogeneities imposed by part build orientation or directional solidification during the AM process. Inspection of L-PBF 17-4 PH SS microstructure has revealed no difference in grain size, grain morphology, or crystallographic orientation within vertically- and horizontally-built samples after heat treatment (solution annealing for 30 min at ~ 1040 °C and peak-aging for 1 h at ~ 482 °C) [11]. Although the microstructures were almost homogenized after heat treatment, the L-PBF 17-4 PH SS specimens still displayed anisotropy in tensile and fatigue strengths as well as elongation to failure, as shown in Fig. 7 [11]. This figure shows engineering stress–strain curves and fully-reversed ($R_e = -1$) strain–life fatigue experimental data for L-PBF 17-4 PH SS in heat treated condition [11]. Kobryn and Semiatin [24] also reported anisotropic tensile and fatigue behaviors for vertical and horizontal DLD Ti-6Al-4V after stress relieving in a vacuum for 2 h at 700–730 °C. These results suggest that the observed structural anisotropy in AM parts may be more influenced by defects rather than microstructure [24].

Using X-ray computed tomography (CT) and microstructural imaging, the defects within various L-PBF 17-4 PH SS samples have been characterized, revealing the presence of large voids with high aspect ratios (ratio of the largest to the smallest overall dimension of the void). Fig. 8a illustrates the typical porosity within the gage sections of horizontal and vertical L-PBF 17-4 PH SS specimens, detected using X-ray CT [11]. As shown in Fig. 8b, these voids (i.e. un-melted regions) were irregular and slit-shaped, forming mostly between layers due to insufficient fusion or low penetration depth of laser [11]. The orientation of these voids with respect to the loading direction were found to be the main source of the structural anisotropy observed in these vertical and horizontal

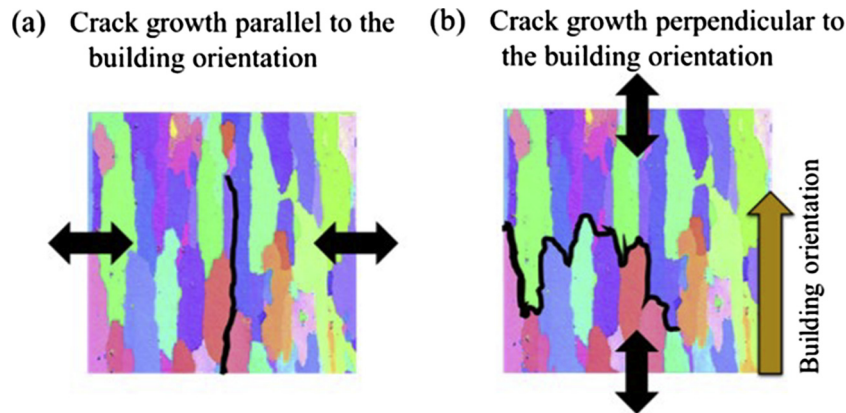


Fig. 6. Schematics demonstrating crack growth (a) parallel and (b) perpendicular to the elongated grains along the building direction (double arrows show the applied loading direction).

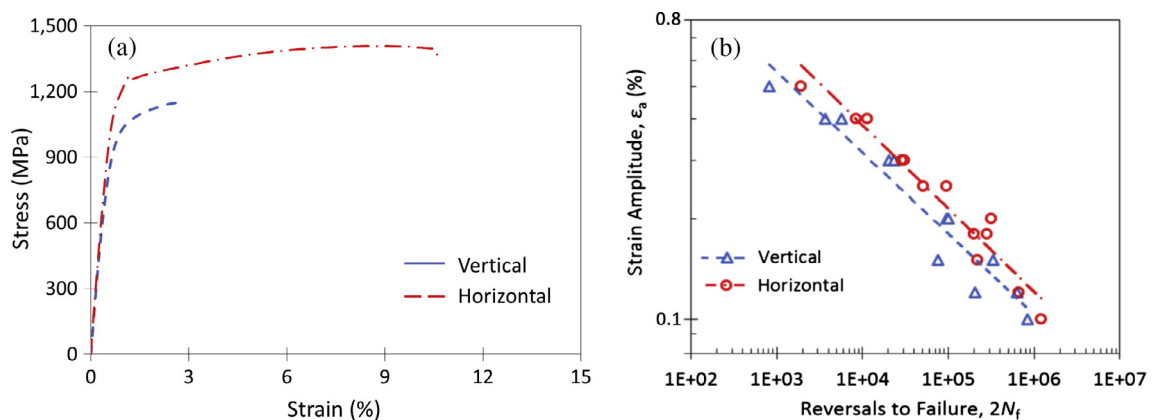


Fig. 7. (a) Engineering stress–strain curves and (b) fully-reversed ($R_c = -1$) strain–life fatigue experimental data for L-PBF 17-4 PH SS, vertically- and horizontally-built, in heat treated condition [11].

specimens, causing anisotropic damage evolution under various loading directions. The lower elongation to failure and fatigue strength of vertical specimens as compared to horizontal ones, as seen in Fig. 7, is most likely due to the fact that the major axes of the split-shaped un-melted regions were perpendicular to the loading axis, thus providing higher stress concentrations, and consequently, easier means for void growth and crack initiation. This is shown schematically in Fig. 8c. For the horizontal specimens, the major axes of the un-melted regions were parallel to the loading direction, resulting in lower stress concentrations and relatively more resistance to crack initiation [11].

Experimental evidence suggests that although the proper heat treatment may be able to remove structural anisotropy arising from microstructure directionality, it may not be a feasible option due to defect directionality. In this regard, the HIP process is a legitimate candidate for remedying structural anisotropies related to microstructure and defects. An investigation on the mechanical behavior of L-PBF Inconel 718 [19] revealed no microstructural (e.g., grain size/morphology, crystallographic orientation) or void directionality (e.g., aspect ratio in shape) within horizontally- and diagonally-built samples after employing HIP. The results of Kobryn and Semiatin [24] have also shown that HIP can significantly reduce the anisotropy in tensile and fatigue properties of DLD Ti-6Al-4V originating from the part's build orientation, by reducing manufacturing-induced porosity, as well as eliminating directional porosities. These results suggest that the high temperature and pressure that occur during a typical HIP process not only

homogenize the microstructure by complete recrystallization of the material [19,29,58], but may also remove or reduce directionality in void shape by decreasing their sharp angles [19,24,59].

Although AM process parameters, such as laser power, scan speed, layer thickness and hatching pitch, can be optimized to obtain almost fully dense parts, as authors herein exercised for L-PBF 17-4 PH SS using immersion method (Archimedes' principle) [11], the use and accuracy of it for improving the structural integrity is at question. The horizontally- and vertically-built L-PBF 17-4 PH SS parts, optimized for density, contained many voids within their gage sections, as can be seen in Fig. 8a. The reason is related to the presence of slit-shaped flaws, i.e. un-melted regions, which covered a broad cross-sectional region with relatively small volume. Therefore, this type of void was not detected via bulk density measurements by immersion method. This indicates that considering only density, as measured by immersion method, as a sole criterion for process parameter optimization may not necessarily lead to the enhanced mechanical properties of AM materials – especially their fatigue resistance [11]. Considering the fact that fatigue failure is a localized structural damage, unlike failure due to static load, presence of a small irregular shaped defect/void close to surface is often enough to cause fatigue failure. However, one small void may not affect the density measurement – using immersion method – significantly.

Fig. 9 shows the effect of heat treatment on fatigue behavior of vertically- and horizontally-built L-PBF 17-4 PH SS specimens [11]. As it can be seen, the heat treated specimens, regardless of their

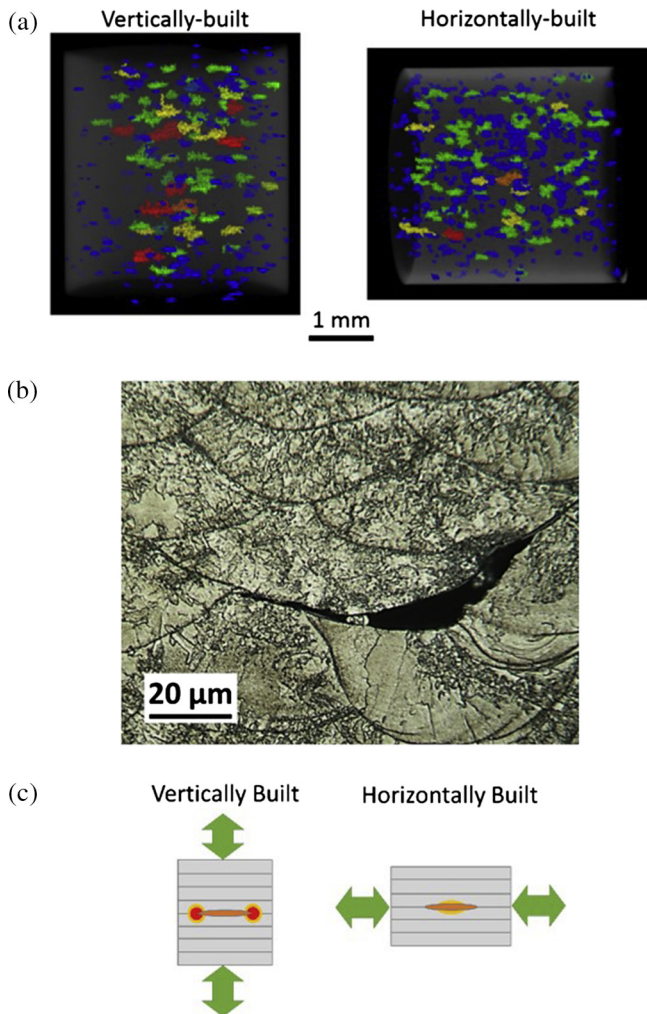


Fig. 8. (a) 3D volumetric image of X-ray CT scan for vertical and horizontal L-PBF 17-4 PH SS specimens showing the void distribution within the gage section (different colors represent different void sizes), (b) radial cross-section images of a horizontal L-PBF 17-4 PH SS specimen in as-built condition, and (c) schematics representing the orientation of a void formed between layers of vertical and horizontal specimens with respect to the loading direction and the resultant stress concentrations [11].

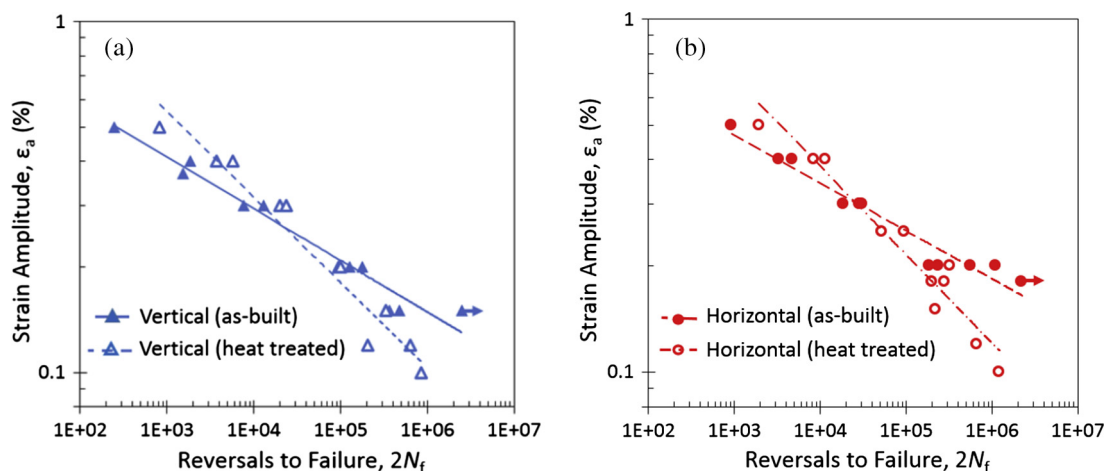


Fig. 9. Fully-reversed ($R_c = -1$) strain-life fatigue experimental data and fits for (a) vertical, and (b) horizontal L-PBF 17-4 PH SS in as-built and heat treated conditions [11].

build orientation, demonstrated higher fatigue strengths relative to their as-built counterparts in LCF. Heat treatment also increased the yield and tensile strengths of both vertically- and horizontally-built specimens [11]. However, contrary to expectation, the heat treated specimens exhibited lower fatigue strength in HCF. For wrought 17-4 PH SS, the HCF strength typically increases after conducting a similar heat treatment schedule due primarily to an increase in tensile strength (or hardness) [60,61]. This is due to the fact that fine, coherent precipitates in the matrix of the heat treated material increase the strength (i.e. tensile strength or hardness), and consequently, cause more resistance to dislocation movement, which results in its enhanced resistance to crack initiation [11]. However, for the AM specimens that already contained voids as large as 100 μm, the mechanism of crack initiation leading to HCF failure has been found to be different.

The more ductile behaving materials are typically less sensitive to impurities, as such materials are accommodating to an increased stress field around their voids through a larger local plastic zone [11,17]. As a result, contrary to their wrought counterparts, heat treating the L-PBF 17-4 PH SS specimens may not improve their fatigue resistance in high cycle regime in the presence of large voids. This suggests that the heat treatment instructions/schedule, found optimal for wrought materials, may not necessarily improve AM part performance. For instance, the specific heat treatment (i.e. solution annealing plus peak-aging), which is beneficial for HCF of wrought 17-4 PH SS, is detrimental for their L-PBF counterparts. Therefore, post-manufacturing processes, such as heat treatment, need to be designed and standardized specifically for AM parts.

5. Effect of surface roughness

Relative to conventionally-manufactured metallic materials, additively-manufactured parts, in as-built condition, possess significantly higher surface roughness, mostly due to partially-melted powder existing along their periphery. This surface roughness has proven to be beneficial for some medical applications (e.g., implants) [62,63]. For instance, the surface roughness of bone-interfacing orthopedic implants may provide better bone in-growth, and consequently, faster and more effective osseointegration – defined as a direct structural and functional connection between living bone and the surface of a load-carrying implant [62,63]. However, surface roughness is one of the most detrimental factors affecting the fatigue performance of metallic materials

under cyclic loading [17,64]. Hence, post-manufacturing operations for improving the durability of AM parts are often required. This is problematic, as many AM parts are desired to be used in their as-fabricated, net-shape condition, especially when they have a complex geometry. Therefore, any post-production surface treatment diminishes a major benefit of AM, i.e. the ability to produce complex geometries in which conventional processing may be impracticable. It is, thus, essential to fully understand the fatigue behavior of AM parts and its dependence on surface finish.

The surface roughness of an AM part can be affected by the type of equipment, powder size, utilized process parameters, and its build orientation [4]. DLD systems typically produce rougher surfaces relative to L-PBF methods, due to their use of thicker hatching pitches and layers, as well as larger size powder. In general, the surface roughness of AM parts typically increases by an increase in hatching pitch, layer thickness, or powder size [4]. Build rate (i.e. laser beam energy or speed) can also affect the surface quality, i.e. as the build rate increases, surface quality decreases [4].

Anisotropic, distinct roughness can also exist along the surface of an AM part. For instance, for a part fabricated via L-PBF while oriented in a vertical incline, the overhanging side (i.e. facing downward toward the build-plate) is found to possess a higher surface roughness relative to the contracting surface (i.e. upward facing side), as shown in Fig. 10 [19,40,65]. This figure presents the X-ray CT image of a 45° orientated Inconel 718 specimen, fabricated via an L-PBF method. Higher surface roughness of the overhanging side is attributed to the more direct contact of this face with the powder bed during manufacture and in this giving rise to melt pool thermal/fluidic edge effects [19]. As with defects and microstructure, the surface roughness varies with respect to position within the part [19,39,66]. It has been found that more near-surface voids form along the downward-facing side of a part fabricated at an incline [19,66], due to melt pool thermal/fluidic edge effects while in contact with powder bed during manufacture, e.g., capillary action, heat build-up, and more [19].

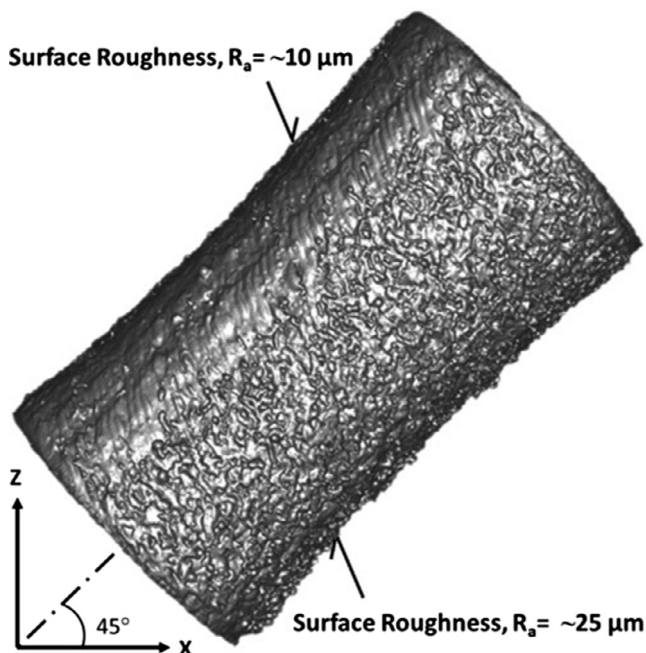


Fig. 10. X-ray CT image of a 45° orientated Inconel 718 specimen, fabricated via an L-PBF method, showing a higher surface roughness for the overhanging side (i.e. downward facing side toward the build-plate) relative to the contracting surface (i.e. upward facing side) [19].

Several studies in the literature have investigated the effect of post-manufacturing surface treatment (e.g., as-built, machined, polished) on the fatigue behavior of various materials [13,18,21,22]. Results generally indicate that reducing the surface roughness, R_a , by machining or polishing, will improve the fatigue resistance of AM materials, especially in the long life regime (i.e. HCF). Spiering et al. [15] showed a higher HCF strength at a stress ratio of $R_\sigma = 0.1$ for machined ($R_a = \sim 5 \mu\text{m}$) L-PBF 316L SS relative to their as-built counterparts ($R_a = \sim 50 \mu\text{m}$). However, the differences in LCF behavior of machined and as-built specimens were found to be small. Stoffregen et al. [25] also studied the effect of surface condition (as-built versus machined) on the HCF behavior of L-PBF 17-4 PH SS under pulsating-tension ($R_\sigma = 0$) loading. Their results revealed a HCF strength for machined specimens ($R_a = \sim 0.6 \mu\text{m}$) nearly twice as high as that of as-built ones ($R_a = \sim 14 \mu\text{m}$). Nevertheless, the fatigue strength of as-built L-PBF 17-4 PH SS tended to meet that of machined one in the mid-life fatigue regime [25]. Results of Aboulkhair et al. [67] showed very close fatigue resistance for as-built ($R_a = \sim 17 \mu\text{m}$) and machined ($R_a = \sim 0.6 \mu\text{m}$) L-PBF AlSi10 Mg specimens under tension-tension loading condition ($R_\sigma = 0.1$) in both mid-life and long-life regimes.

Wycisk et al. [68] studied HCF behavior of Ti-6Al-4V fabricated via L-PBF under as-built ($R_a = \sim 12 \mu\text{m}$) and polished conditions at a stress ratio of $R_\sigma = 0.1$. Their results exhibited a significantly lower HCF strength (i.e. endurance limit) for as-built specimens (210 MPa) relative to their polished counterparts (500 MPa) [68]. In addition, contrary to expectation, they reported higher scatter in the HCF region for polished specimens as compared to as-built specimens [68]. This can be explained by differences in crack initiation mechanisms between as-built and polished specimens. Analysis of fatigue fracture surfaces revealed crack initiation from surface discontinuities for the as-built specimens, whereas polished specimens showed failure from both surface roughness and interior defects [68]. These results suggest that the differences in defect type, size, and location, serving as a crack initiation site for polished specimens, may cause scatter in HCF data. In general, the influence of surface finish on fatigue behavior of AM parts may also be affected by material type, particularly its ductility and involved failure mechanisms. A more ductile behaving material exhibits less sensitivity to defects, surface roughness, or any stress raiser features in the microstructure. Accordingly, different materials, or even the same material with different post-manufacturing heat treatments, may show distinct sensitivity to surface machining – depending on crack initiation mechanisms (e.g., surface versus sub-surface).

Edward and Ramala [29] investigated the effect of surface finish (as-built versus machined) on the fatigue behavior of L-PBF Ti-6Al-4V fabricated in different build orientations under $R_\sigma = -0.2$ loading. They reported higher surface roughness and surface tensile residual stress for the specimens fabricated in the vertical orientation ($R_a = \sim 38 \mu\text{m}$) relative to their horizontally-oriented counterparts ($R_a = \sim 31 \mu\text{m}$) [29]. Therefore, it can be expected that the vertically-built specimens exhibit a larger difference between the as-built and machined conditions, as the higher surface roughness and surface tensile residual stress are more detrimental to fatigue resistance by accelerating the crack initiation stage. However, contrary to these expectations, their results showed that the effect of surface machining on improving part's HCF resistance was more pronounced for specimens fabricated in a horizontal orientation as compared to the vertical orientation [29]. This can be explained by considering the crack initiation mechanism as well as presence of sub-surface voids, their size and distribution. Analysis of fatigue fracture surfaces, conducted in [29], revealed the presence of large sub-surface un-melted regions ($>100 \mu\text{m}$). By machining and removing the rough surface, these sub-surface voids are brought

to the surface of the specimens. Thus, these surface voids can still serve as a crack initiation site and affect the part's fatigue behavior. In addition, depending on the size and shape, these surface voids may be more detrimental than surface roughness as they can provide a higher stress concentration. Un-melted regions are more detrimental for vertically-built specimens relative to horizontally-built ones, as shown in Fig. 8, due to their wider projected area and larger stress concentration. As a result, the fatigue behavior of vertically- and horizontally-built specimens with respect to post-AM surface machining may vary based on the characteristics of interior voids formed during fabrication.

The fatigue behavior of Inconel 718 fabricated via L-PBF has been recently investigated [19]. Experimental results have indicated that the location of interior voids and the thickness of the outer layer that is removed during machining are important parameters when quantifying the effects of surface finish (i.e. as-built versus machined) on fatigue behavior of AM parts. In this particular study, the room-temperature uniaxial fatigue behavior of L-PBF Inconel 718 – stress relieved, HIPed (at $1163\text{ °C} \pm 10\text{ °C}$ and $\sim 102\text{ MPa}$ for 3 h), solution treated, and aged – were investigated under as-built ($R_a = \sim 20\text{ }\mu\text{m}$) and machined ($R_a = \sim 2\text{ }\mu\text{m}$) conditions [19]. It is worth noting that for the as-built specimens (i.e. fabricated directly in their net shape configuration), the circumferential surface roughness introduced error when measuring the gage section diameter, as depicted in Fig. 11. Therefore, it is essential to consider the effective load carrying area (i.e. aggregate area) for calculating the actual applied stress and comparing the fatigue behavior of as-built and machined specimens.

The stress amplitude versus fatigue life, obtained from fully-reversed ($R_\sigma = -1$) fatigue tests, of the L-PBF Inconel 718 specimens in the machined and as-built conditions are shown in Fig. 12 [19]. It may be seen that as-built specimens have similar fatigue resistance relative to their machined counterparts in both LCF and HCF regimes. Typically, it is expected that the as-built specimens with rougher surface condition show significantly lower fatigue resistance relative to machined specimens, at least in HCF regime, where crack initiation often dominates the total fatigue lifetime. However, the above scenario was not observed in this study, and this is most likely due to the presence of sub-surface large voids, which were brought to the surface by machining [19].

Analysis of the fatigue fracture surfaces revealed that surface voids or discontinuities were the most life-limiting features of both machined and as-built L-PBF Inconel 718 specimens, regardless of the life regime (i.e. LCF or HCF) [19]. This is due to the fact that defects at the surface can provide higher stress concentration,

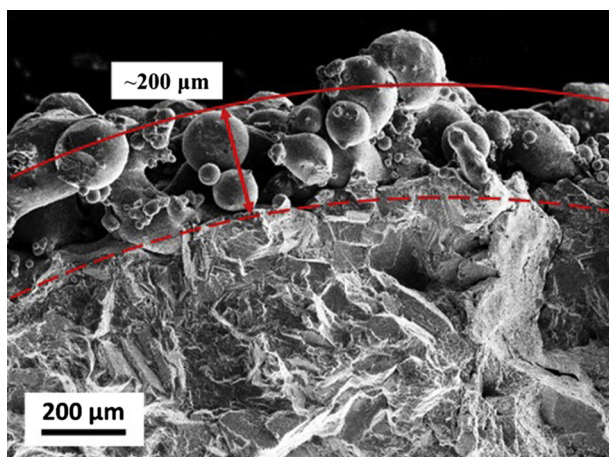


Fig. 11. Presence of partially-melted powders on gage section of as-built specimens, causing errors during measurement of fatigue specimens' diameter. The specimen's diameter is approximately 5 mm.

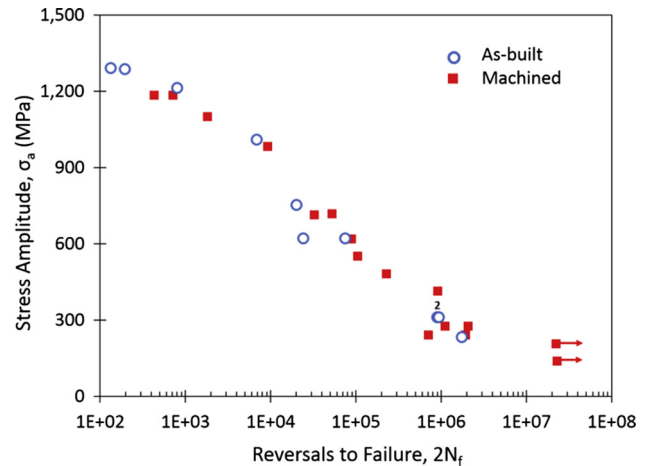


Fig. 12. Room temperature fully-reversed ($R_\sigma = -1$) uniaxial fatigue stress-life data for L-PBF Inconel 718 in machined and as-built conditions [19].

leading to earlier crack initiation. In addition, cracks tend to grow faster along the free surface relative to the depth of the part [69].

The short-life and early mid-life failure mechanisms of both machined and as-built L-PBF Inconel 718 specimens were characterized with cracks initiating from multiple damage sites [19]. This can be explained by the fact that the crack growth life is a larger fraction of the total fatigue life at higher stress levels (i.e. LCF), which provides an opportunity for other cracks to initiate [70,71]. In long life fatigue regimes, large voids on the surface of machined specimens were found to always serve as crack initiation sites. In this case, the most 'severe' void near the surface controls the fatigue life of machined specimens and typically, a single, dominant crack grows to failure [19].

Multiple crack initiation sites, however, were found on the fatigue fracture surfaces of the as-built specimens that failed during HCF. This is attributed to the existence of more potential fatigue crack initiation sites on the surface of as-built specimens, due to the existence of a large number of discontinuities on the specimen outer surface [19]. Accordingly, several regions with similar conditions (i.e. size, location, etc.) can serve as possible crack initiation sites. As a result, crack initiation and propagation from multiple sites were observed for as-built specimens instead of crack initiation and propagation from the most extreme, life-limiting void that was observed for machined specimens. However, since the effects of crack propagation and coalescence are not as significant in this regime, no major differences can be noticed in Fig. 12 for fatigue lives between the machined and as-built specimens at HCF [19].

The X-ray CT scans, taken from the gage section of an as-built L-PBF Inconel 718 specimen, revealed the presence of large voids along the perimeter, as can be seen in Fig. 13a. Direct contact of the part's surface with the powder bed during manufacture may have given rise to melt pool thermal/fluidic edge effects (i.e. instabilities), leading to near-surface voids along the edges of the part. In addition, the HIP process cannot remove open voids (i.e. surface-connected voids) because these type of voids act as an extension of the specimen's surface [72]. Therefore, for as-built L-PBF parts, the probability of voids being near the surfaces is higher than machined ones. These observations suggest that the thickness of material removed during machining may play a significant role on the fatigue behavior of post-machined AM parts. In other words, depending on the thickness of the outer layer that is trimmed away during machining, the voids may be removed or brought to the surface. As a result, fatigue behavior of machined specimens may be different based on the specimen design, as shown in Fig. 13b.

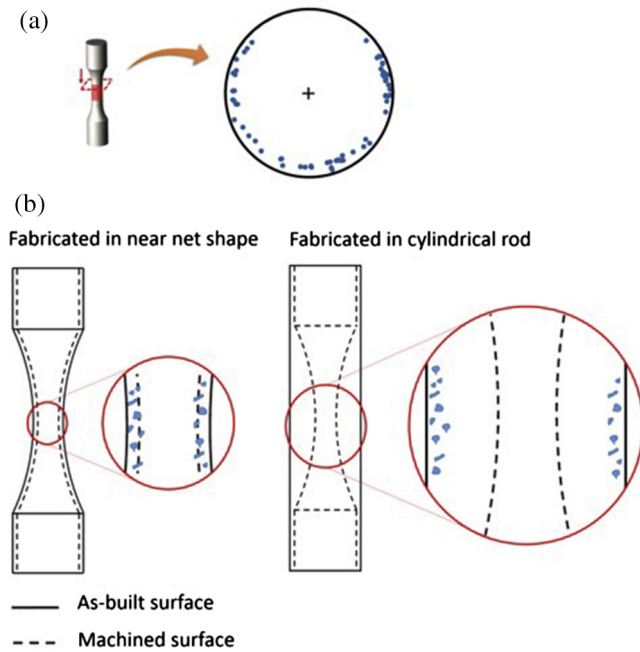


Fig. 13. (a) Distribution of voids mapped on the cross sectional view of a gage section, captured by X-ray CT scan of an as-built specimen [19], and (b) schematics showing different specimen designs, including fabricating the near net shape specimen or cylindrical rod.

Fig. 13b schematically shows different specimen designs, including fabricating the near net shape specimen as well as cylindrical rod. As seen, the thickness of the outer layer that needs to be trimmed away during machining is thinner for the near net shape specimen as compared to the rod one. Accordingly, by removing a thin layer from the surface of a near net shape fabricated specimen, the effect of surface machining on fatigue life may not be as pronounced [19]. These findings suggest that the specimen design procedure may need to be standardized for AM materials in order to obtain a better understanding of their fatigue behavior as it pertains to the more robust engineering of parts fabricated via AM. However, if the process/design parameters are optimized in such a way that there are no near surface voids in the as-built specimens, the thickness of the removed layer during the post-manufacturing machining process should not greatly affect the fatigue behavior.

6. Some immediate opportunities

The fatigue behavior and related challenges inherent to metallic parts fabricated via laser-based AM has been summarized and discussed. However, there are many more challenges related to the improvement of AM parts that have not been discussed in this overview, such as residual stress, very high cycle fatigue behavior, process parameter optimization, process control, and more. Regardless, it has been clearly demonstrated that the fatigue resistance of AM parts is typically lower than their wrought counterparts mainly due to presence of manufacturing induced defects. Furthermore, material properties obtained from laboratory specimens may not be directly applicable for determination of part performance.

Laboratory specimens experience a thermal history unique to their own fabrication and different to that of parts. As a result, microstructural features and mechanical properties obtained from laboratory specimens and actual parts are also expected to be different. Therefore, it is essential to establish process-structure-prop

erty-performance relationships of AM materials in order to reduce uncertainty in predicting the performance of fabricated parts. In addition, mechanical testing methods and specimen design procedures may need to be revised to better understand the mechanical behavior of engineering parts fabricated via AM. Post-manufacturing treatment protocols used for wrought materials may not be applicable for improving the durability of AM materials. Thus, procedures for the effective and consistent post-manufacturing treatments of wrought materials may need to be revised for AM parts.

Addressing the aforementioned challenges can only be accomplished by a better understanding of the interrelationships among process parameters, thermal history, solidification, resultant microstructure, and mechanical behavior of AM parts, as presented schematically in Fig. 14 [9]. As seen, utilized process and design parameters affect the thermal history (i.e. cooling rate, thermal gradients, and cyclic reheating) of the AM part. The thermal history during fabrication governs solidification, and consequently, all the resultant microstructural details such as grain size, morphology, and orientation; defect size, type, and distribution; residual stress, etc. Accordingly, these microstructural features dictate the structural properties, and especially the fatigue performance, of fabricated parts.

It is clear that the machine-to-machine and process variability can complicate the understanding of interrelationships between process/design parameters and ultimate AM part performance. Therefore, one solution for ensuring the adoption of AM materials for application should center on predicting the variations in mechanical behavior of AM parts based on their resultant microstructure. The AM process parameters for a specific material system and AM method need to be ultimately optimized based on the geometry/size of the part as well as for achieving the desired/targeted mechanical properties. In addition, improving the fatigue resistance may be possible by aligning the best conceivable properties of a part in accordance with the loading characteristics/directions and/or minimizing the defects in the part's critical locations with high stresses. These opportunities in additive manufacturing of materials with better fatigue resistance materials are discussed in more details in the following sections.

6.1. Microstructural sensitive mechanical models

Variations of microstructural details resulting from AM processing conditions cause greater uncertainty and scatter in mechanical behavior, and especially the fatigue resistance, of AM parts. Despite significant research efforts toward optimizing process parameters to fabricate AM parts with uniform microstructure [2,10], overcoming this challenge is still an open issue. Achieving a homogeneous, defect free AM product immediately after its fabrication has not yet been fully demonstrated. Therefore, having the ability to accurately predict variation in mechanical behavior may accelerate the adoption of AM for a myriad of engineering applications. In this regard, a microstructural sensitive mechanical model that can incorporate the microstructural details, especially defect statistics (e.g., size and spacing), may be appropriate for modeling the mechanical behavior of AM parts [9]. Such a microstructure-property model provides the ability to predict damage evolution under loading – whether monotonic or cyclic fatigue – based on the microstructural details resulting from the manufacturing process.

The internal state variable (ISV) plasticity-damage model [73,74] is an example of such microstructural sensitive mechanical models and has proven to be effective in linking microstructural details (i.e. grain size and morphology as well as defects statistics) to deformation behavior of materials under tension, compression, and torsion loading conditions. This model incorporates the main

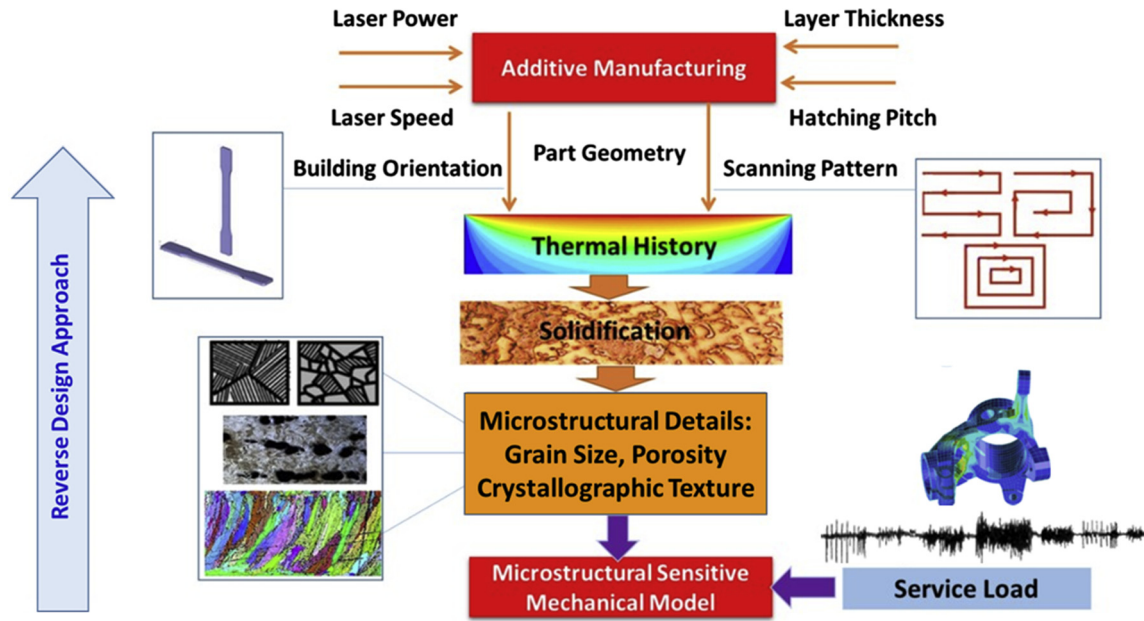


Fig. 14. Relationships among manufacturing process parameters, thermal history, solidification, microstructure, and mechanical behavior of AM parts [9].

steps related to damage evolution, i.e. void nucleation, growth, and coalescence to predict the monotonic stress-strain response of the material as well as its variations as affected by microstructural properties and defects statistics.

The applicability of the ISV plasticity-damage model to predict the monotonic tensile behavior of DLD 316L SS was examined by the authors herein [75]. In this particular study [75], the effects of microstructural features, associated with the manufacturing process of both ‘single-built’ and ‘multi-built’ DLD 316L SS (see Fig. 3) on stress-strain behavior were successfully captured using the ISV plasticity-damage model. Fig. 15 presents the stress-strain data from tension experiments and the predictions based on the ISV plasticity-damage model for single-built and multi-built DLD 316L SS [75]. The predicted lower and upper bounds, presented in Fig. 15, indicate that the model is capable of capturing scatter in stress-strain experimental data (shown as error bars) using the microstructural details unique to each set of specimens. The ranges observed during tension experiments for elongation to

failures were predicted using the defects data/statistics in the fabricated material. The ranges for yield and ultimate strengths were also determined by the standard deviation of measured grain size in each set [75].

Under cyclic loading, the multi-stage fatigue (MSF) model, as introduced by McDowell et al. [76], can be a useful microstructural sensitive fatigue model as it has a proven ability to capture microstructural details and to link them to fatigue behavior. The MSF model considers multiple experimentally-observed stages of fatigue damage evolution, i.e. crack incubation, small crack growth, and long crack growth. The MSF model was successfully applied to DLD 316L SS [77] and DLD Ti-6Al-4V [78], as shown in Fig. 16. The fatigue behavior in these materials can be modeled based on microstructural features, such as grain size, porosity, void size and spacing.

This specific model (i.e. MSF model) also has the ability to provide a range of possible fatigue lives depending on the microstructural properties and defects, as presented in Fig. 16 [77,78]. Analysis of fatigue fracture surfaces has revealed that fatigue cracks are mostly initiated from relatively large voids located at or near the specimens’ surface [77,78]. Thus, the lower and upper bounds correspond to the largest and smallest void diameters observed and this aids in predicting uncertainty in the fatigue experimental data. As seen from Fig. 16, these bounds fit the data satisfactorily, with most of the experimental data points falling within the upper and lower prediction bounds. More importantly, the upper bounds predicted by the MSF model are also close to the fitted curves for wrought materials, as can be seen from Fig. 16, indicating that the void size is a significant contributor to the fatigue behavior of DLD 316L SS [77,78]. In other words, the model correctly predicts the fatigue behavior of the wrought material close to the upper bound, where voids are either very small or do not even exist.

Although such microstructural sensitive fatigue models are difficult to calibrate, they are very useful for AM parts as they do not have uniform microstructural properties and defects statistics, due to variation of thermal history in different locations of the part. Therefore, it may be worth calibrating the model once, although experimentally exhaustive, and then using it for any element/point of the part only by knowing the microstructural details (e.g., grain

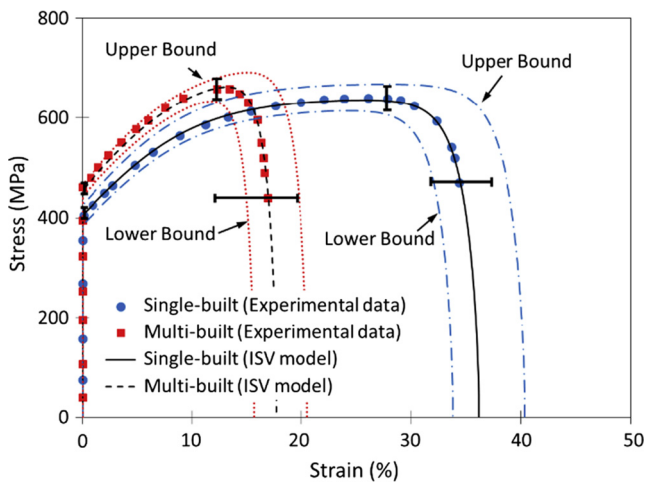


Fig. 15. ISV plasticity-damage model predictions of lower and upper bounds as compared with the experimental data and scatter bands (shown by error bars) for single-built and multi-built DLD 316L SS [75].

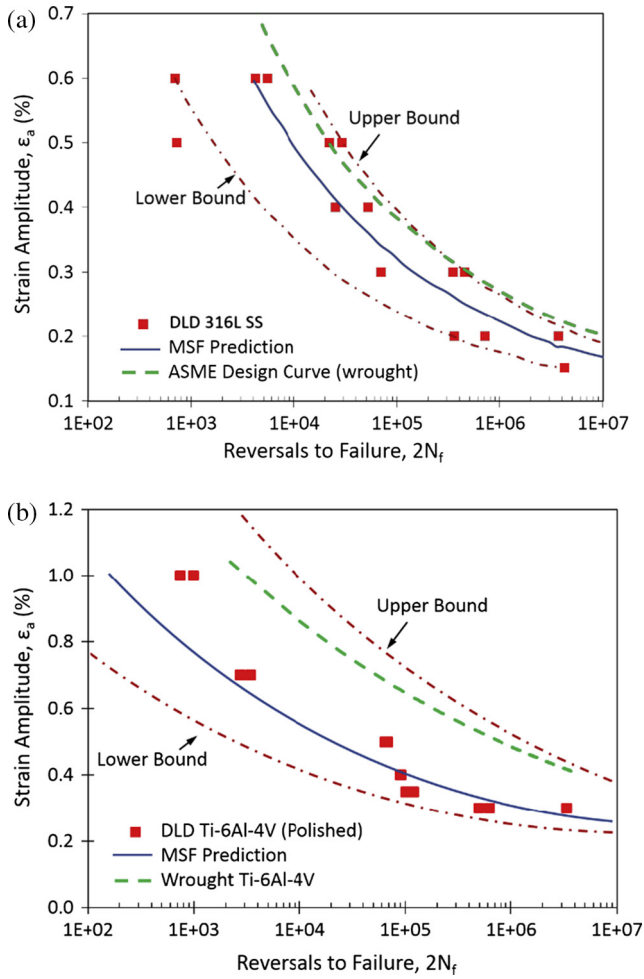


Fig. 16. Fatigue life predictions using a microstructural sensitive fatigue model for (a) DLD 316L SS [77], and (b) DLD Ti-6Al-4V [78] data. Experimental strain life fatigue curves for conventionally-built materials [23,82] are also superimposed.

size and defects statistics). These models provide a means for predicting the mechanical behavior by linking the stress/strain (based on geometry and loading) and strength (based on microstructure and defects properties) contours.

6.2. Design for application

6.2.1. Critical location(s) approach

Developing microstructural sensitive mechanical models based on structure-property relationships of AM materials would be the first step toward minimizing costly prototyping, reducing testing, design optimization, and improving part reliability. Such models can also be complemented by using finite element analysis (FEA) to determine the critical location(s) or element(s) with higher stress/strain and possibility of fatigue failure for any part with a complex geometry. As a result, a reverse design approach can be developed to determine process/design parameters based on the targeted application, geometry, and service loading, as shown in Fig. 14.

After determining the critical location(s) and associated stress/strain for a part via FEA, the performance of the AM part may be enhanced by appropriately tuning/selecting the process and design parameters for the critical location(s) with high stresses. For the real-time controllable AM systems, defects can be minimized at critical location(s) through controlling process and design parameters during fabrication, as described schematically in Fig. 14, by

means of a reverse engineering approach. This approach is much more time and cost efficient than controlling the process for the entire part. For AM methods lacking a real-time monitoring and controlling system, the most suitable process parameters can be selected based on the critical location(s) geometry. In this case, the local thermal histories dictate the most appropriate process parameters for fabricating a part, with minimal defects at critical location(s). Therefore, thermal simulations of the AM process in advance of fabrication can help in adjusting the process/design parameters to achieve the desired thermal history [79]. However, enhancing the mechanical performance by adjusting the process/design parameters, even at critical locations, requires an understanding of process-structure-property-performance relationships of AM materials and parts.

Improving the surface quality only for the critical location(s) would be an alternative approach to enhance fatigue performance of AM structural components under service loading. The need for post-manufacturing surface treatment (e.g., machining, polishing, shot-peening, or laser shock peening) limits the appeal of AM technology, which provides the ability to produce complex geometries unachievable via conventional manufacturing methods. Hence, conducting post-manufacturing surface treatments only on the critical location(s) would be more efficient and better justified for parts manufactured by AM techniques.

6.2.2. Critical direction(s) approach

Strategically aligning the relative orientation of a material's strongest plane(s) to the loading critical direction(s) in parts is another solution for improving the fatigue performance of AM parts. In other words, the inherent anisotropy of AM materials may provide a unique opportunity to improve their fatigue performance through texture control; by matching the most critical stressing direction(s) within the part to the best properties offered by texture. This may include defining an appropriate angle between layers – linked to the grain morphology, crystallographic orientation, and voids' directionality – and loading direction.

A combination of experimental, computational, and analytical methods may be utilized to facilitate an approach, as shown schematically in Fig. 17, for designing parts with enhanced structural integrity under service loading. The left side of the “V” defines the loading requirements as stress/strain histories at the critical element(s)/location(s) dictated by the part geometry and realistic, multiaxial loading; while the right side of the “V” describes the design approach to fabricate materials with the desired

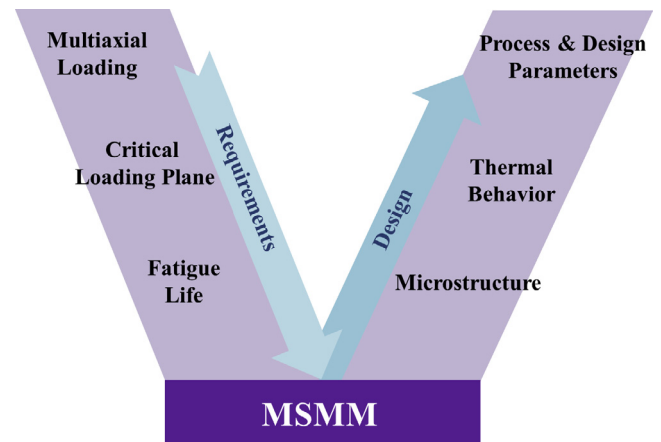


Fig. 17. The approach introduced to design fabricated AM parts with enhanced structural integrity under general service loading. MSMM stands for microstructural sensitive mechanical models.

microstructure, including grain size and orientation as well as defects distribution and directions.

The multiaxial stresses in critical elements of components and structures not only arise from multidirectional loading, stress concentrations, or residual stresses [80], but also from the heterogeneity of the microstructure, specifically for AM materials. Therefore, it is essential to account for the cyclic multiaxial stresses/strains in design by a means of an appropriate multiaxial fatigue model. Multiaxial loadings can be categorized as either in-phase (IP) or out-of-phase (OP). For IP or proportional loading, the ratio of torsional to axial loading and its principal directions remain fixed; under OP or non-proportional loading, principal directions, and consequently, maximum shear directions, rotate in time.

Investigations of cracking behavior under multiaxial loading indicate that cracks usually nucleate on preferred planes within the material, as presented in Fig. 18 for 1050 normalized steel under IP loading [60]. Although the preferred orientation depends on the material and the state of loading, it can be seen from Fig. 18 that such orientation is not random. This suggests that the preferred plane(s) for cracks can be detected based on damage distribution on all planes within the material, assuming the material is isotropic and homogenous, using an appropriate multiaxial damage parameter.

Damage observations suggest critical plane approaches, which reflect the physical mechanism of the fatigue damage process, are most reliable and robust for multiaxial fatigue life estimations [80]. These approaches consider specific plane(s) within the material with maximum fatigue damage as the critical plane(s). The Fatemi-Socie (FS) model [81] is an example of a critical plane approach for shear damage materials, as presented by Eq. (1):

$$\frac{\Delta\gamma_{\max}}{2} \left(1 + k \frac{\sigma_{n,\max}}{\sigma_y} \right) = C \quad (1)$$

where σ_y is the material monotonic yield stress and k is the material constant, which can be found by fitting uniaxial fatigue data to the torsion fatigue data, $\Delta\gamma_{\max}/2$ is the maximum shear strain amplitude and $\sigma_{n,\max}$ is the normal stress acting on the plane of maximum shear strain.

An example of damage distribution with plane orientation for IP and 90° OP axial-torsion loading with the same equivalent strain based on the FS parameter is shown in Fig. 19 [80]. As seen, a higher damage value for OP loading results in a shorter fatigue life as compared to IP loading. More importantly, the maximum damage values, based on FS damage parameter, occur along the 115°

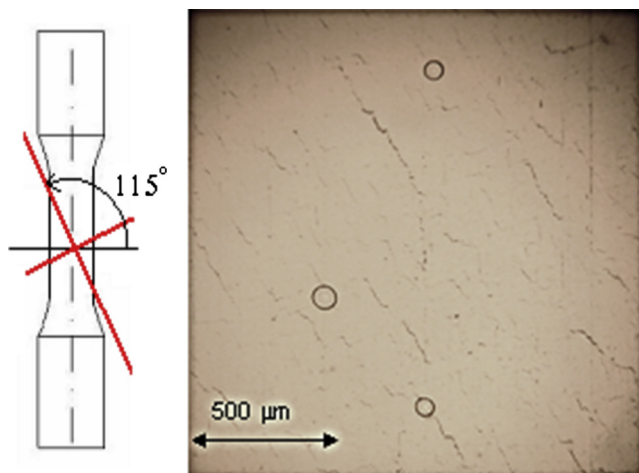


Fig. 18. Preferred cracking orientation observed for 1050 normalized steel under in-phase (IP) axial-torsion loading [60].

and 0° planes for IP and OP loadings, respectively – in agreement with experimental observation for cracking orientations, shown in Fig. 19. Results indicate that cracks nucleate and grow on the plane(s) with the highest damage values, depending on the material and the state of loading, rather than random orientation.

It should be noted that this may not be the case for AM materials considering the fact that they are often anisotropic due to their texture and defects' directionality, respectively, resulting from the presence of elongated grain morphology and inter-layer slit-shaped voids. For AM materials, which are not necessarily homogeneous and isotropic, a relative critical plane approach needs to be defined to account for both material and loading critical planes. In this case, the relative critical plane approach can be utilized for the reverse engineering, based on Fig. 17, to align the strongest material plane with the loading critical plane, and the weakest material plane with the direction which experiences minimum damage from loading.

The multiaxial fatigue life of AM parts can possibly be improved by the development of directionally processed materials in which the best property/texture directions are aligned with the most critical loading plane under service loading. By performing analytical critical plane searches in the macroscale, the directions with high risk of fatigue failure under multiaxial loading can be determined. A microstructural sensitive fatigue model can then relate the damage values in different directions to microstructural properties (i.e. grain morphology, crystallographic orientation, and defect orientation) for the intended service loading and the required life cycle. Thereupon, the obtained relationship may be utilized to adjust the process and design parameters to control the thermal history for desired microstructure (grain morphology, crystallographic orientation, and defects' directionality), as shown in Fig. 17, to move the material's critical plane (i.e. weak plane) from the loading critical plane. The required thermal history, including cooling and solidification rates and heat flux direction, can also be simulated for predicting and/or controlling appropriate process/design parameters during or before AM, as needed.

For instance, as seen from Fig. 19, if loading is IP, the strongest plane should be aligned with ~15° or ~115° planes and the weakest aligned with ~65° or ~155° planes. Similarly, if the loading is OP, the strongest plane should be aligned with 0° plane and the weakest plane to fall somewhere within 50–130° range. These techniques, including critical locations and directions as well as microstructural sensitive mechanical models, may provide a means of fabricating more fatigue resistant AM parts until fabrication of defect free products can be fully achieved.

7. Summary

While AM continues to demonstrate potential for full-scale production of customized and/or complex parts, the mechanical behavior, and thus, trustworthiness of these parts is not yet well understood. This creates a challenge for AM technology to be fully adopted in various engineering applications such as aerospace, automotive, and biomedical. To overcome this challenge, the process-structure-property-performance relationships for various AM processes (e.g., laser powder bed fusion and direct laser deposition) and material systems must be established. Since the fabrication parameters (process) of AM parts affect their microstructure (structure), which dictates the mechanical behavior (property) and the part performance, it is imperative that all of these phases be taken into consideration.

Despite numerous experimental research efforts focused on characterizing the fatigue behavior of AM metals over the past decade, more research is required to enable more accurate and reliable fatigue life estimation methodologies for AM parts. This particular

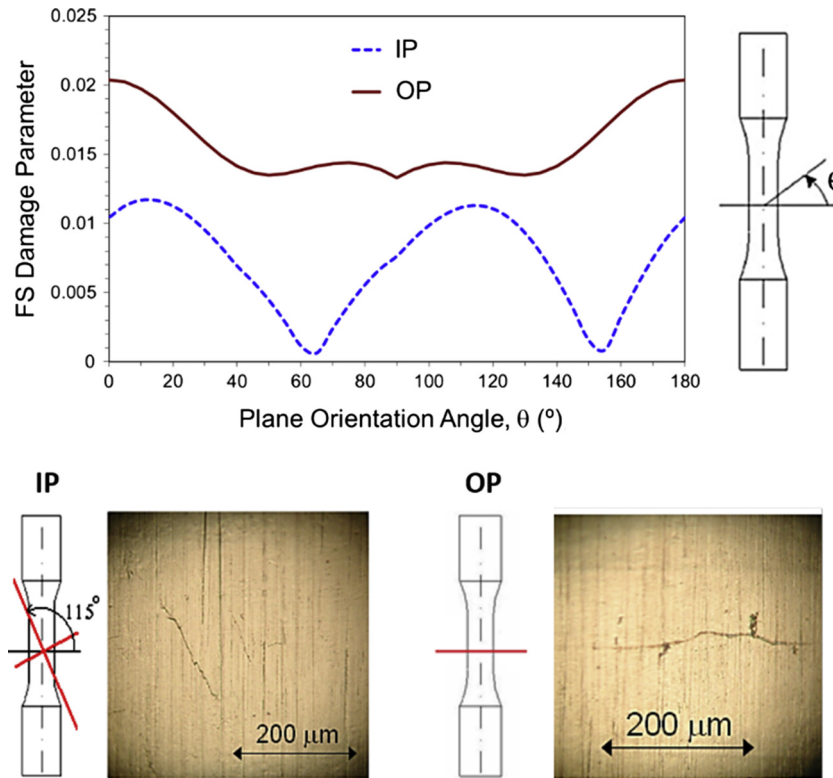


Fig. 19. Variation of FS damage parameter with plane orientation under in-phase (IP) and 90° out-of-phase (OP) axial-torsion loadings at the same strain levels [80]. The observed cracking orientations are also demonstrated.

problem is challenging and demands standardized approaches and measurement techniques. This overview paper has discussed several important ongoing challenges related to the fatigue of AM materials. Some possible, immediate solutions have been also presented as a means to provide insights into overcoming some of the challenges related to the structural integrity of AM parts.

Fatigue and durability evaluation are among the major challenges against widespread adoption of AM parts. In general, damage evolution of metallic AM materials under cyclic loading conditions is directly affected by impurities sourced from the AM process itself. Among the many different sources of damage evolution under cyclic loadings, voids are the major life limiting factor and the most dominant mechanism for fatigue crack initiation in AM metals. Variations in location, shape, and size of voids are found to be the main reason for the large scatter in the AM fatigue data. The HIP process can be used to improve the durability and HCF performance of AM parts by fusing un-melted particles, decreasing the voids size and smoothening their sharp angles, and even closing some voids. However, it should be noted that employing the HIP process in order to improve the fatigue resistance may not necessarily lead to the same outcome for different AM materials. In addition to the parameters chosen for HIP (i.e. pressure and temperature), material microstructure, associated failure mechanism, void location, and the encapsulated gas inside of the voids play important roles.

Any change in the size, geometry, or number of fabricated parts on the build plate may significantly affect the inter-layer time intervals and thermal dissipation during AM process. The experienced thermal history, and consequently, the resultant microstructure and mechanical properties of the fabricated parts strongly depend on their size and geometry. Therefore, due to variations in thermal histories, specimen properties may not be directly applicable to determine/predict the part performance. In addition,

for a part with complex geometry, a homogenous microstructure and defect distribution is hard to achieve via current laser-based AM methods.

The build orientation of AM parts can generate anisotropic structural response, especially in fatigue behavior. This is attributed to the microstructure (i.e. grain morphology and crystallographic orientation) and defect directionality (i.e. distinct dimensions of the void in different planes). High temperature and pressure during the HIP process may significantly reduce the anisotropy in structural properties of AM parts, imposed by build orientation, via homogenizing the microstructure through complete recrystallization of the material, as well as removing the directionality in void shape by smoothening their sharp angles.

Comparing the results of various studies suggests that the influence of surface finish on fatigue behavior of materials may also be affected by material type, particularly its ductility and involved failure mechanisms. In addition, void characteristics – especially their locations – and the thickness of the removed surface during machining may play significant roles on the fatigue behavior of machined AM parts. Depending on the thickness of the outer layer that is trimmed away during machining, the voids may be removed or brought to the surface. Thus, fatigue behavior of machined specimens may be different based on the specimen design.

Mechanical testing methods, design procedures, standards, etc. may need to be revised for AM materials. Difficulty of relating specimen properties to the part performance, due to different thermal history, also needs to be addressed in the mechanical testing methods and design procedures. In addition, the structural integrity of AM parts may not necessarily improve following the heat treatment schedule found effective for wrought materials, due to the unique fatigue failure mechanisms of AM metallic parts. Therefore, post-manufacturing processes (e.g., heat treatment) also need to be developed specifically for AM parts.

Although microstructural sensitive mechanical models are difficult to calibrate, they may be suitable for AM parts, as they possess variations in microstructural properties and defects statistics, resulting from unique thermal histories experienced at different locations within a part. Providing the ability to predict the variation in mechanical behavior based on the microstructural details, such models may be beneficial for reducing prototype testing, as well as improving the part's reliability and design optimization. Microstructural sensitive mechanical models can also be complemented by using finite element analysis (FEA) to determine the critical location(s) with high probability for fatigue failure. Therefore, enhancing the fatigue resistance of AM parts may be more economically possible by improving the surface quality and minimizing defects only in these critical location(s).

In addition, turning the weak plane in the material (i.e. material critical direction) away from the loading critical direction in the component may be another solution for improving fatigue performance of AM parts, considering their anisotropic and nonhomogeneous properties. By determining the directions with high risk of fatigue failure under the intended service loading, appropriate microstructural and defect properties, in particular orientation, can be identified to tolerate the loading by a means of a microstructural sensitive fatigue model. Finally, the obtained relationship may be utilized to adjust the process and design parameters to control the thermal history for achieving the desired microstructural and defects' directionalities. Again, this requires an understanding of process-structure-property-performance relationships of AM materials.

Acknowledgement

This material is based upon work supported by the National Science Foundation under Grant No. 1657195.

References

- [1] ASTM. ASTM Standard F2792-12a: Standard terminology for additive manufacturing technologies; 2012.
- [2] Thompson SM, Bian L, Shamsaei N, Yadollahi A. An overview of direct laser deposition for additive manufacturing; Part I: Transport phenomena, modeling, and diagnostics. *Addit Manuf* 2015;8:36–62.
- [3] Selcuk C. Laser metal deposition for powder metallurgy parts. *Powder Metall* 2011;54:94–9.
- [4] Frazier WE. Metal additive manufacturing: a review. *J Mater Eng Perform* 2014;23:1917–28.
- [5] Lott P, Schleifenbaum H, Meiners W, Wissenbach K, Hinke C, Bültmann J. Design of an optical system for the in situ process monitoring of selective laser melting (SLM). *Phys Procedia* 2011;12:683–90.
- [6] Emelogu A, Marufuzzaman M, Thompson SM, Shamsaei N, Bian L. Additive manufacturing of biomedical implants: a feasibility assessment via supply-chain cost analysis. *Addit Manuf* 2016;11:97–113.
- [7] Levy G, Schindel R, Kruth J. Rapid manufacturing and rapid tooling with layer manufacturing (LM) technologies, state of the art and future perspectives. *CIRP Ann Technol* 2003;2:589–609.
- [8] Murr LE, Gaytan SM, Medina F, Lopez H, Martinez E, Machado BI, et al. Next-generation biomedical implants using additive manufacturing of complex, cellular and functional mesh arrays. *Philos Trans R Soc A Math Phys Eng Sci* 2010;368:1999–2032.
- [9] Shamsaei N, Yadollahi A, Bian L, Thompson SM. An overview of direct laser deposition for additive manufacturing; Part II: Mechanical behavior, process parameter optimization and control. *Addit Manuf* 2015;8:12–35.
- [10] Aboutaleb A, Bian L, Elwany A, Shamsaei N, Thompson S, Tapia G. Accelerated process optimization for laser-based additive manufacturing by leveraging prior studies. *IE Trans* 2016. <http://dx.doi.org/10.1080/0740817X.2016.1189629>.
- [11] Yadollahi A, Shamsaei N, Thompson MS, Elwany A, Bian L. Effects of building orientation and heat treatment on fatigue behavior of selective laser melted 17-4 PH stainless steel. *Int J Fatigue* 2017;94:218–35.
- [12] Yadollahi A, Shamsaei N, Thompson SM, Seely D. Effects of process time interval and heat treatment on the mechanical and microstructural properties of direct laser deposited 316L stainless steel. *Mater Sci Eng, A* 2015;644:171–83.
- [13] Daniewicz SR, Shamsaei N. An introduction to the fatigue and fracture behavior of additive manufactured parts. *Int J Fatigue* 2017;94:167.
- [14] Bian L, Thompson SM, Shamsaei N. Mechanical properties and microstructural features of direct laser deposited Ti-6Al-4V. *JOM* 2015;67:629–38.
- [15] Spierings AB, Starr TL, Wegener K. Fatigue performance of additive manufactured metallic parts. *Rapid Prototyp J* 2013;19:88–94.
- [16] Troesch T, Strößner J, Völkl R, Glatzel U. Microstructure and mechanical properties of selective laser melted Inconel 718 compared to forging and casting. *Mater Lett* 2016;164:428–31.
- [17] Stephens RI, Fatemi A, Stephens RR, Fuchs HO. *Metal fatigue in engineering*. 2nd ed. Wiley; 2000.
- [18] Sterling A, Torries B, Shamsaei N, Thompson SM, Seely DW. Fatigue behavior and failure mechanisms of direct laser deposited Ti-6Al-4V. *Mater Sci Eng, A* 2016;655:100–12.
- [19] Yadollahi A, Shamsaei N, Wells DN, Daniewicz SR. Fatigue behavior and failure analysis of additive manufactured Inconel 718 superalloy [under preparation].
- [20] Halford GR. *Fatigue and durability of structural materials*. ASM International; 2006.
- [21] Ma X, Duan Z, Shi H, Murai R, Yanagisawa E. Fatigue and fracture behavior of nickel-based superalloy Inconel 718 up to the very high cycle regime. *J Zhejiang Univ Sci A* 2010;11:727–37.
- [22] Leybold HA. Axial-load fatigue tests on 17-7 PH stainless steel under constant-amplitude loading. *NASA Tech Note* 19980228273; 1960.
- [23] Carrion P, Shamsaei N. Strain-based fatigue data for Ti-6Al-4V ELI under fully-reversed and mean strain loads. *Data Br* 2016;7:12–5.
- [24] Kobryn PA, Semiatin SL. Mechanical properties of laser-deposited Ti-6Al-4V. In: *Solid free fabr proceedings*, Austin, p. 179–86.
- [25] Stoffregen HA, Butterweck K, Eberhard Abele. Fatigue analysis in selective laser melting: review and investigation of thin-walled actuator housings. In: *Solid free fabr symp*. p. 635–50.
- [26] Bagheri A, Mahtabi M, Shamsaei N. Fatigue behavior and cyclic deformation of additive manufactured NiTi [submitted for publication].
- [27] Leuders S, Vollmer M, Brenne F, Tröster T, Niendorf T. Fatigue strength prediction for titanium alloy TiAl6V4 manufactured by selective laser melting. *Metall Mater Trans A* 2015;46:3816–23.
- [28] Mahtabi MJ, Shamsaei N, Mitchell M. Fatigue of nitinol: the state-of-the-art and ongoing challenges. *J Mech Behav Biomed Mater* 2015;50:228–54.
- [29] Edwards P, Ramulu M. Fatigue performance evaluation of selective laser melted Ti-6Al-4V. *Mater Sci Eng, A* 2014;598:327–37.
- [30] Leuders S, Thöne M, Riemer A, Niendorf T, Tröster T, Richard HA, et al. On the mechanical behaviour of titanium alloy TiAl6V4 manufactured by selective laser melting: fatigue resistance and crack growth performance. *Int J Fatigue* 2013;48:300–7.
- [31] Kasperovich G, Hausmann J. Improvement of fatigue resistance and ductility of TiAl6V4 processed by selective laser melting. *J Mater Process Technol* 2015;220:202–14.
- [32] Leuders S, Lienenke T, Lammers S, Tröster T, Niendorf T. On the fatigue properties of metals manufactured by selective laser melting – the role of ductility. *J Mater Res* 2014;29:1911–9.
- [33] Boom R, Kamperman AA, Dankert O, Veen A. Argon solubility in liquid steel. *Metall Mater Trans B* 2000;31:913–9.
- [34] Mahmoudi M, Elwany A, Yadollahi A, Thompson S, Bian L, Shamsaei N. Mechanical properties and microstructural characterization of selective laser melted 17-4 PH stainless steel. *Rapid Prototyp J* 2016.
- [35] Torries B, Shao S, Shamsaei N, Thompson S. Effect of inter-layer time interval on the mechanical behavior of direct laser deposited Ti-6Al-4V. In: *Solid free fabr proc*.
- [36] Nicoletto G. Anisotropic high cycle fatigue behavior of Ti-6Al-4V obtained by powder bed laser fusion. *Int J Fatigue* 2017;94:255–62.
- [37] Simonelli M, Tse YY, Tuck C. Effect of the build orientation on the mechanical properties and fracture modes of SLM Ti-6Al-4V. *Mater Sci Eng, A* 2014;616:1–11.
- [38] Niendorf T, Leuders S, Riemer A, Richard HA, Tröster T, Schwarze D. Highly anisotropic steel processed by selective laser melting. *Metall Mater Trans B* 2013;44:794–6.
- [39] Li P, Warner DH, Fatemi A, Phan N. Critical assessment of the fatigue performance of additively manufactured Ti-6Al-4V and perspective for future research. *Int J Fatigue* 2016;85:130–43.
- [40] Shrestha R, Sirmsiriwong J, Shamsaei N, Thompson N, Bian L. Effect of build orientation on the fatigue behavior of stainless steel 316L via a laser-based powder bed fusion process. In: *Solid free fabr proc*.
- [41] Mower TM, Long MJ. Mechanical behavior of additive manufactured, powder-bed laser-fused materials. *Mater Sci Eng, A* 2015;651:198–213.
- [42] Zhang D, Niu W, Cao X, Liu Z. Effect of standard heat treatment on the microstructure and mechanical properties of hot isostatically pressed superalloy Inconel 718. *Mater Sci Eng, A* 2015;644:32–40.
- [43] Carter LN, Martin C, Withers PJ, Attallah MM. The influence of the laser scan strategy on grain structure and cracking behaviour in SLM powder-bed fabricated nickel superalloy. *J Alloys Compd* 2014;615:338–47.
- [44] Pilchak AL, Bhattacharjee A, Williams REA, Williams JC. The effect of microstructure on fatigue crack initiation in Ti-6Al-4V. *ICF12*, vol. 2; 2013. p. 1–10.
- [45] Bantounas I, Lindley TC, Rugg D, Dye D. Effect of microtexture on fatigue cracking in Ti-6Al-4V. *Acta Mater* 2007;55:5655–65.
- [46] Evans W, Jones J, Whittaker M. Texture effects under tension and torsion loading conditions in titanium alloys. *Int J Fatigue* 2005;27:1244–50.
- [47] Bache MR. Processing titanium alloys for optimum fatigue performance. *Int J Fatigue* 1999;21:105–11.

- [48] Sinha V, Mills MJ, Williams JC, Spowart JE. Observations on the faceted initiation site in the Dwell-fatigue tested Ti-6242 alloy: crystallographic orientation and size effects. *Metall Mater Trans A* 2006;37:1507–18.
- [49] Sackett E, Germain L, Bache M. Crystal plasticity, fatigue crack initiation and fatigue performance of advanced titanium alloys. *Int J Fatigue* 2007;29:2015–21.
- [50] Peters M, Gysler A, Lütjering G. Influence of texture on fatigue properties of Ti-6Al-4V. *Metall Trans A* 1984;15:1597–605.
- [51] Bantounas I, Dye D, Lindley TC. The effect of grain orientation on fracture morphology during high-cycle fatigue of Ti-6Al-4V. *Acta Mater* 2009;57:3584–95.
- [52] Hall JA. Fatigue crack initiation in alpha-beta titanium alloys. *Int J Fatigue* 1998;19:23–37.
- [53] Zhai T, Wilkinson AJ, Martin JW. A crystallographic mechanism for fatigue crack propagation through grain boundaries. *Acta Mater* 2000;48:4917–27.
- [54] Jiang XP, Man C-S, Shepard MJ, Zhai T. Effects of shot-peening and re-shot-peening on four-point bend fatigue behavior of Ti-6Al-4V. *Mater Sci Eng, A* 2007;468–470:137–43.
- [55] Pilchak AL, Williams RE, Williams JC. Crystallography of fatigue crack initiation and growth in fully lamellar Ti-6Al-4V. *Metall Mater Trans A* 2009;41:106–24.
- [56] Riemer A, Leuders S, Thöne M, Richard HA, Tröster T, Niendorf T. On the fatigue crack growth behavior in 316L stainless steel manufactured by selective laser melting. *Eng Fract Mech* 2014;120:15–25.
- [57] Konečná R, Kunz L, Nicoletto G, Bača A. Fatigue crack growth behavior of Inconel 718 produced by selective laser melting. *Frat Ed Integrità Strutt* 2016;35:31–40.
- [58] Chang SH. In situ TEM observation of γ' , γ'' and δ precipitations on Inconel 718 superalloy through HIP treatment. *J Alloys Compd* 2009;486:716–21.
- [59] Zhang YP, Yuan B, Zeng MQ, Chung CY, Zhang XP. High porosity and large pore size shape memory alloys fabricated by using pore-forming agent (NH_4HCO_3) and capsule-free hot isostatic pressing. *J Mater Process Technol* 2007;192–193:439–42.
- [60] Shamsaei N, Fatemi A. Effect of hardness on multiaxial fatigue behaviour and some simple approximations for steels. *Fatigue Fract Eng Mater Struct* 2009;32:631–46.
- [61] Wu J, Lin C. Tensile and fatigue properties of 17-4 PH stainless steel at high temperatures. *Metall Mater Trans A* 2002;33:1715–24.
- [62] Anil S, Anand PS, Alghamdi H, Jansen JA. Dental implant surface enhancement and osseointegration. *InTech Open Access Publ* 2011:83–108.
- [63] Shalabi MM, Gortemaker A, Van't Hof MA. Surface roughness and bone healing: a systematic review. *J Dent Res* 2006;85:496–500.
- [64] Kovoacevic R, Jamshidinia M, Kong F PA, Semiati SL. The numerical modeling of fatigue properties of a bio-compatible dental implant produced by electron beam melting (EBM). In: *Proceeding solid free fabr symp*. p. 791–804.
- [65] Fox JC, Moylan SP, Lane BM. Effect of process parameters on the surface roughness of overhanging structures in laser powder bed fusion additive manufacturing. *Procedia CIRP* 2016;45:131–4.
- [66] Beretta S, Romano S. A comparison of fatigue strength sensitivity to defects for materials manufactured by AM or traditional processes. *Int J Fatigue* 2017;94:178–91.
- [67] Aboulkhair NT, Maskery I, Tuck C, Ashcroft I, Everitt NM. Improving the fatigue behaviour of a selectively laser melted aluminium alloy: Influence of heat treatment and surface quality. *Materials & Design* 2016;104:174–82.
- [68] Wycisk E, Solbach A, Siddique S, Herzog D, Walther F, Emmelmann C. Effects of defects in laser additive manufactured Ti-6Al-4V on fatigue properties. *Phys Procedia* 2014;56:371–8.
- [69] Xie W, Yang H, Su X, Huang Q. Numerical simulation of fatigue crack growth of surface crack. *ISMME* 2014:56–61.
- [70] Shamsaei N. Multiaxial fatigue and deformation including non-proportional and variable amplitude loading effects. University of Toledo; 2010.
- [71] Shamsaei N, Fatemi A. Small fatigue crack growth under multiaxial stresses. *Int J Fatigue* 2014;58:126–35.
- [72] Atkinson HV, Davies S. Fundamental aspects of hot isostatic pressing: an overview. *Metall Mater Trans A* 2000;31:2981–3000.
- [73] Bammann DJ, Aifantis EC. A damage model for ductile metals. *Nucl Eng Des* 1989;116:355–62.
- [74] Bammann DJ. An internal variable model of viscoplasticity. *Int J Eng Sci* 1984;22:1041–53.
- [75] Yadollahi A, Shamsaei N, Hammi Y, Horstemeyer MF. Quantification of tensile damage evolution in additive manufactured austenitic stainless steels. *Mater Sci Eng, A* 2016;657:399–405.
- [76] McDowell DL, Gall K, Horstemeyer MF, Fan J. Microstructure-based fatigue modeling of cast A356-T6 alloy. *Eng Fract Mech* 2003;70:49–80.
- [77] Xue Y, Pascu A, Horstemeyer MF, Wang L, Wang PT. Microporosity effects on cyclic plasticity and fatigue of LENSTM-processed steel. *Acta Mater* 2010;58:4029–38.
- [78] Torries B, Sterling AJ, Shamsaei N, Thompson SM, Daniewicz SR. Utilization of a microstructure sensitive fatigue model for additively manufactured Ti-6Al-4V. *Rapid Prototype* 2016;22:817–25.
- [79] Masoomi M, Gao X, Thompson SM, Shamsaei N, Bian L, Elwany A. Modeling, simulation and experimental validation of heat transfer during selective laser melting. *ASME/IMECE*; 2015.
- [80] Fatemi A, Shamsaei N. Multiaxial fatigue: an overview and some approximation models for life estimation. *Int J Fatigue* 2011;33:948–58.
- [81] Fatemi A, Socie DF. A critical plane approach to multiaxial fatigue damage including out-of-phase loading. *Fatigue Fract Eng Mater Struct* 1988;11:149–65.
- [82] Strizak JP, Tian H, Liaw PK, Mansur LK. Fatigue properties of type 316LN stainless steel in air and mercury. *J Nucl Mater* 2005;343:134–44.

Glossary

3D: three-dimensional
 AM: additive manufacturing
 CT: computed tomography
 DLD: direct laser deposition
 FS: Fatemi-Socie
 HCF: high cycle fatigue
 HIP: hot isostatic pressing
 IP: in-phase
 ISV: internal state variable
 LCF: low cycle fatigue
 LENS: laser engineered net shaping
 L-PBF: laser powder bed fusion
 MSF: multi-stage fatigue
 OP: out-of-phase
 PBF: powder bed fusion
 PH: precipitation hardening
 SLM: selective laser melting
 SS: stainless steel